

FACULTY OF TECHNOLOGY  
SOUTHAMPTON INSTITUTE

---

FINAL YEAR DISSERTATION

BENG (HONS) YACHT AND POWERCRAFT DESIGN

NICOLAS ROUSSELON

VOLVO OPEN 70 WITH INVESTIGATION  
INTO HULL AND APPENDAGES DESIGN

MAY 2004

This project is submitted in part fulfilment of the Degree of  
**Bachelor of Engineering with Honours in Yacht & Powercraft Design**  
at the Southampton Institute  
in May 2004

## ACKNOWLEDGMENT

The author would like to thank the following people:

- Mr. Wallis (Author's tutor) for its help and availability through the project
- Mr. Barkley for its help on the towing tank and the Vpp regression process
- All the towing tank staff
- Vincent Laine for being project/building manager of the towing tank model

## ABSTRACT

The main aim of the project is to investigate the hull and appendages design on a Volvo Open 70. These boats are designed to a new rule, a therefore much work is currently being done on these boats. The author was particularly interested in comparing the present project results and the boats that will be built soon using the best design tools and people. In academic terms, the project was used to increase the author knowledge in hydrodynamic and structures, using advanced tools and processes.

Hull design was done with input from advanced VPP work with a detailed weight and weather study. The weather study was used to class the boat. The detailed weight estimate enabled an accurate influence of beam on the overall weight.

Appendages design was done with input from experimental (towing tank) and numerical work. The towing tank tests involved testing two different configurations that form past experience and theory appeared to be best. The best configurations was then refined using numerical tools and common sense.

It was found that best hull/appendages configuration for the Volvo Ocean race 2005 would be a hull at the maximum displacement to maximise bulb weight with a appendages configuration where the lift (side force) is generated by two foils situated aft and forward of the keel.

# CONTENTS

<b>Acknowledgment</b>	p 02
<b>Abstract</b>	p 02
<b>Contents</b>	p 03
<b>00 - Nomenclature</b>	p 07
<b>01 - Introduction</b>	p 08
<b>02 - Volvo ocean race</b>	p 09
02.1 The rule	
02.2 The race	
<b>03 - Weather study</b>	p 11
<b>04 - Weight and centres estimate</b>	p 12
04.1 Introduction	p 12
04.2 Influence of beam on structural weight	p 12
04.3 Influence of beam on rig weight	p 12
04.4 Influence of bulb weight on fin weight	p 12
04.5 Choices affecting weight estimate	p 13
<b>05 - Hull design</b>	p 14
05.1 Introduction	p 14
05.2 Preliminary Hull design – Bwl iterations in Vpp	p 14
05.3 Systematic series: Beam investigation	p 15
05.4 Midship section	p 17
05.4.1 Shearline, freeboards	
05.4.2 Small angle Stability issue	
05.5 Hull design for specific speeds and heel	p 18
05.5.1 Optimisation of Cp and LCB	
05.5.2 Assumptions of the method, problems	
05.6 Towing tank input	p 21
05.7 Conclusion	p 21
<b>06 - VPP configuration</b>	p 22
06.1 VPP 3.X	
06.2 VPP 4.X	
06.3 Common file	
06.4 Resistance added in waves (RAW)	
<b>07 - Appendages design</b>	p 24
07.1 Introduction	p 24
07.2 Bulb design	p 25
07.2.1 Overview	p 25
07.2.2 Computational Fluid Dynamic	p 25
07.2.3 Preliminary Bulb shape	p 26

07.2.3.1 Assumptions, main aspects	p 26
07.2.3.2 Length	p 28
07.2.3.2 Cross section shape	p 28
07.2.3.2.1 Relation Centre of gravity – Increase of drag bulb	
07.2.3.2.2 Height/Breadth ratio	
07.2.4 Computational tool aided design	p 30
07.2.5 Conclusion	p 31
07.3 Rudders	p 33
07.3.1 Introduction	p 33
07.3.2 System advantages: theory	p 33
07.3.3 System advantages: practice	p 33
07.3.3.1 Main aspects	
07.3.3.2 Longitudinal balance	
07.3.4 Longitudinal position of the rudders	p 34
07.3.5 Rudder sections	p 35
07.3.6 Rudders area	p 36
07.3.7 Rudder planform	p 37
07.3.7.1 Overview: rudder interaction	p 37
07.3.7.2 Forward rudder	p 37
07.3.7.3 Aft rudder	p 38
07.3.7.3.1 Introduction	
07.3.7.3.2 Lifting line	
07.3.7.3.3 Conclusion	
07.3.8 Viscous interaction	p 42
07.3.8.1 Introduction	
07.3.8.2 Investigation	
07.3.9 Structural design	p 43
07.3.10 Conclusion	p 44
07.4 Canting Keel	p 45
07.4.1 Introduction	p 45
07.4.2 The rule	p 45
07.4.3 Lateral area requirement	p 45
07.4.4 Keel section thickness choice	p 46
07.4.5 Structural requirement	p 47
07.4.6 Keel fillet	p 48
07.4.7 Planform shape	p 48
07.4.8 Canting keel mechanism	p 49
07.4.9 Practical consideration	p 49
07.4.10 Conclusion	p 49
<b>08 - Towing tank</b>	p 50
08.1 Introduction	p 50

08.2 Model used	p 50
08.3 Model design	p 51
08.4 Appendages tested	p 51
08.5 Extrapolation	p 52
08.6 Canting keel influence on upright resistance	p 53
08.7 Influence of forward rudders on wave resistance	p 53
08.8 Conclusion	p 53
<b>09 - VPP investigation</b>	p 55
09.1 Resistance breakdown in WinVPP	p 55
09.2 Comparison of the two configurations	p 56
09.2.1 Change of daggerboard area and rudders area	p 56
09.2.2 Results	p 57
09.3 Discussion	p 60
09.4 Choice of appendages	p 60
<b>10 - Rig design</b>	p 61
10.1 The rule	p 61
10.2 Choice	p 61
10.3 Structure	p 61
10.4 Weight Influence	p 62
<b>11 - Sail design</b>	p 63
11.1 The rule	p 63
11.2 Choice	p 63
11.3 Design	p 64
<b>12 - Hull Structural design</b>	p 65
12.1 Rule	p 65
12.2 Design	p 65
12.2.1 Primary load influence	p 66
12.2.1.1 Load estimation	p 66
12.2.1.2 EI calculations	p 66
12.2.1.3 Deflection	p 66
12.2.1.4 Results	p 67
<b>13 - Deck Plan</b>	p 68
<b>14 - General Arrangement</b>	p 68
<b>15 - Stability check</b>	p 69
15.1 Damaged stability	p 69
15.2 Angle of vanishing stability	p 70
<b>16 - Conclusion</b>	p 71
<b>17 - References</b>	p 72
<b>18 - Bibliography</b>	p 73
<b>19 - Appendices</b>	p 74
Weather study	p A1

Weight and centres estimate		p A2
Hydrostatic data		p A3
Lifting Line code		p A4
Rudder stock structure		p A6
Keel calcs		p A8
Towing tank		p A9
VPP comparison		p A9
Rig Design		p A10
Sail design		p A11
ABS Internal calcs sample		p A12
Hull Structural design: Deflection		p A14
<b>Plans</b>		p 91
VO70-LP1	Lines Plan	p 92
VO70-A1-1	Appendages plan : Rudders	p 93
VO70-A1-2	Appendages plan : Keel + Bulb	p 94
VO70-A1-3	Appendages plan : Arrangement	p 95
VO70-SPDP1	Sail and deck plan	p 96
VO70-SBF1	Structure BHD and frames plan	p 97
VO70-SGA1	Structural arrangement plan	p 98
VO70-LS1	Laminate Schedule	p 99
VO70-GA1	General Arrangement	p 100

## 0 - Nomenclature

<b>A</b>	Area	<b>HBI</b>	Height of base of I above water plane
<b>a</b>	Angle of attack	<b>Ig</b>	Fore sail hoist
<b>ABS</b>	American Bureau of Shipping	<b>I</b>	Second moment of inertia
<b>ARe</b>	effective aspect ratio	<b>IMS</b>	International Measurement System
<b>ARg</b>	geometric aspect ratio	<b>k<sub>CB</sub></b>	Hull Form factor
<b>AWA</b>	Apparent wind angle	<b>L/B</b>	Length to Beam ratio
<b>AWS</b>	Apparent wind velocity	<b>LCB</b>	Longitudinal Center of Buoyancy
<b>WA</b>	Waterplane area	<b>LCF</b>	Longitudinal Centre of Flotation
<b>b</b>	Span	<b>LCG</b>	Longitudinal Center of Gravity
<b>BAS</b>	Boom height above sheer line	<b>LOA</b>	Length Overall
<b>BAW</b>	Apparent wind angle	<b>L<sub>WL</sub></b>	Length at the Waterline loaded for race start
<b>Bhd</b>	Bulkhead	<b>μ</b>	Kinematic viscosity
<b>BOA</b>	Beam Overall	<b>NACA</b>	National Advisory Committee for Aeronautics
<b>βt</b>	True wind angle	<b>P</b>	Mainsail hoist
<b>BTR</b>	Beam to draft ratio (B/TC)	<b>q</b>	Dynamic head ( $0.5 * \rho * v^2$ )
<b>Bwl</b>	Waterline beam	<b>ρ</b>	Density
<b>c</b>	Chord length	<b>R.O.R.C.</b>	Royal Offshore Racing Club
<b>Cd</b>	Local Drag coefficient (2-D)	<b>RANSE</b>	Reynolds averaged Navier Stokes Equation
<b>C<sub>D</sub></b>	Total drag coefficient (3-D)	<b>RAW</b>	Added resistance in waves
<b>C<sub>ai</sub></b>	Induced drag coefficient	<b>reef</b>	Sail Reef parameter
<b>Cdp</b>	Parasitic drag coefficient	<b>Rf</b>	Frictional resistance
<b>CE</b>	Aerodynamic centre of effort	<b>R<sub>H</sub></b>	Resistance due to heel
<b>C<sub>F</sub></b>	Friction coefficient	<b>R<sub>I</sub></b>	Induced resistance
<b>C<sub>L</sub></b>	Total Lift coefficient (3-D)	<b>RM</b>	Righting moment
<b>C<sub>l</sub></b>	Local lift coefficient (2-D)	<b>R<sub>N</sub></b>	Reynolds number
<b>CLR</b>	centre of lateral resistance	<b>Rr</b>	Residuary resistance
<b>CoG</b>	Centre of Gravity	<b>R<sub>T</sub></b>	Total resistance
<b>Cp</b>	Prismatic Coefficient	<b>R<sub>U</sub></b>	Upright resistance
<b>C<sub>R</sub></b>	Root chord	<b>T</b>	Maximum draft
<b>C<sub>T</sub></b>	Tip chord	<b>t/c</b>	Thickness chord ratio
<b>Disp</b>	Displacement	<b>Tc</b>	Canoe body draft
<b>DSYHS</b>	Delft Systematic Yacht Hull Series	<b>TCG</b>	Transversal centre of gravity
<b>DWL</b>	design waterline	<b>Te</b>	Effective draft
<b>E</b>	Mainsail foot length	<b>UD</b>	Unidirectional
<b>SAC</b>	Section Area Curve	<b>Vb</b>	Boat Velocity
<b>S<sub>D</sub></b>	Section drag	<b>v</b>	Speed
<b>SF</b>	Sideforce	<b>Vol</b>	Volume of displacement
<b>f(a,b)</b>	Function of parameters a and b	<b>V.C.G</b>	Vertical Centre of Gravity
<b>FEA</b>	Finite Element analysis	<b>VCG</b>	Vertical centre of gravity
<b>Ff</b>	Freeboard at the stem	<b>VMG</b>	Velocity Made Good ( $Vb * \cos(BAW)$ )
<b>FH</b>	Heeling Force (Normal to mast)	<b>VOR70</b>	Volvo open 70
<b>flat</b>	Sail Flat Parameter	<b>VPP</b>	Velocity Prediction Program
<b>F<sub>N</sub></b>	Froude Number	<b>TWS</b>	True wind velocity
<b>FoS</b>	Factor of Safety	<b>TWA</b>	True wind angle
<b>FRP</b>	Fibre Reinforced Plastic	<b>WA</b>	Waterplane area
<b>g</b>	acceleration due to gravity (taken as 9.81 m/s <sup>2</sup> )	<b>WSA</b>	Wetted surface area (canoe body only)
<b>GM</b>	Metacentric height	<b>ZCE</b>	Vertical centre of effort position above water plan
<b>GZ</b>	righting arm	<b>Z</b>	Section modulus

## 01 - Introduction

The main aim of this project is the design of a Volvo Open 70. Coverage of the full design process is not possible in the limited time available. The author made the decision to focus his research on the optimization of the hull and appendages. The main parts affecting hull and appendages design have been studied thoroughly with the help of advanced tools (Towing tank and CFD).

Due to the limited space available (100 pages), the author has not developed the general theory developed in class or already assessed in the year. (e.g.; tank testing scaling, etc). The amateur reader should refer to general yacht design or aerodynamic books for details.

The considerable dimension of the project implied a cautious management. Time schedules and design flow charts have been used to assist the whole process.

## 02 - Volvo Ocean Race

### 02.1 The rule [1] [2]

"The starting point is a brand new, state of the art, 70' monohull race-boat. This open design will have a canting keel and a choice of multiple rudders / daggerboards. Above all, it will be very fast and exciting to sail. The prescribed rule will remain relatively open, presenting a challenge and test for designers. The new Volvo Open 70 will be an easier boat to sail, with fewer sails to handle and better living conditions for the crew. The race rules will favour imagination, creativity and sailing skills, and not an environment where the biggest purse necessarily gives a bigger edge." So touts the organizers of the Volvo Ocean Race.

The main parameters of the hull are; a maximum length of 21.5 m, a beam between 4.7 and 5.7 m, a draft of 4.5 m, at least 4500 kg in the bulb, a light displacement of 12500 kg. Yachts will have an open choice of multiple rudder / daggerboard options, the restriction being that each appendage can only have one degree of freedom (rotation, retraction, etc.)

A canting keel is required and aft ballast tank filled without electric is permitted.

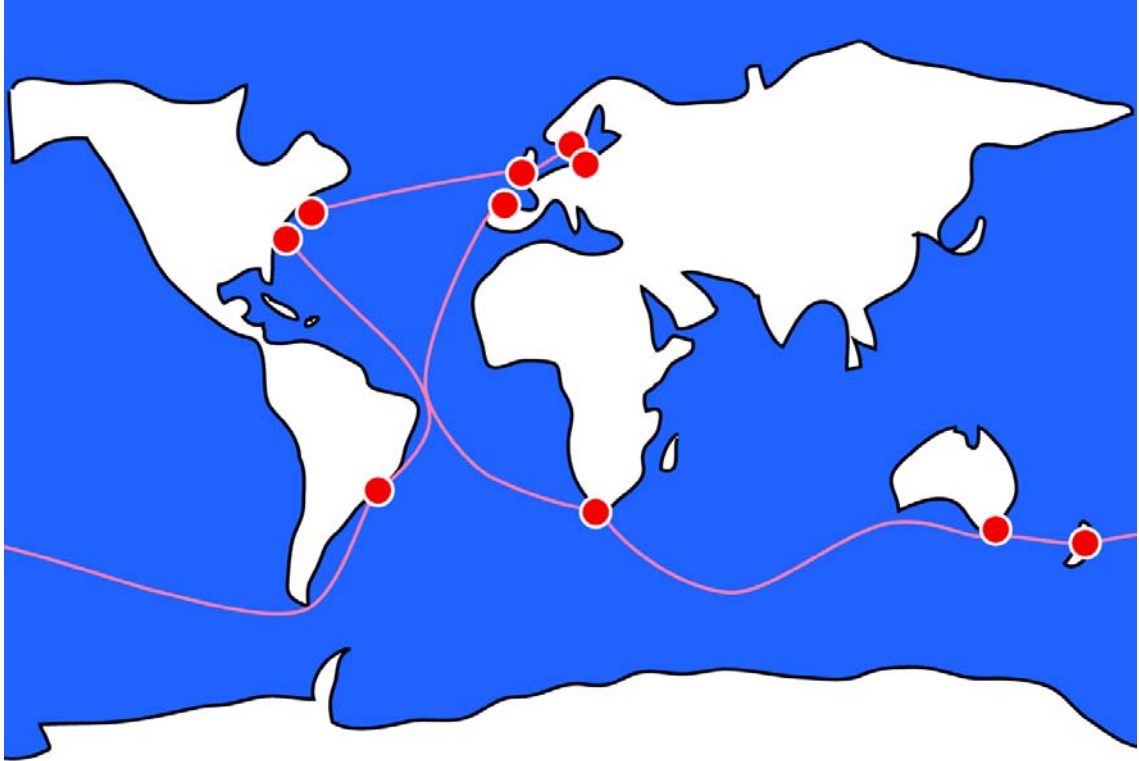
The rule is relatively open. No girth measurement is linked with Lwl as in the Volvo 60 rule. The rule is a development of the successful open 60s with more restrictions to have boats with similar potential the first time out.

### 02.2 The race

This culmination of creativity and innovation has given birth to the Volvo 70 and a new format of racing that couples long-distance offshore sailing with six action-packed inshore stopovers. Starting from Vigo in Spain on November 5th, 2005, the race ports-of-call include Cape Town/South Africa, Melbourne/Australia, Rio de Janeiro/Brazil, Baltimore/Annapolis/USA, Southampton/UK, Gothenburg/Sweden, and a finish at a Baltic port (TBA).

The race will be scored on a high-point system tiered to the number of competing yachts. Using 12 entries as an example: On each of the seven ocean legs, 1st, 2nd, 3rd placed finishers will receive 12, 11, 10 points, respectively. Mid-ocean scoring gates (one or two per leg) add an additional 6, 5.5, 5 points to the 1st, 2nd, 3rd boats to round these locations. And each of the six in-port regattas will award 1st, 2nd, 3rd

placed finishers with 6, 5.5, 5 points, respectively. The ocean legs will account for 80% of the total point tally, while in-port, round-the-cans sprints will account for 20%.



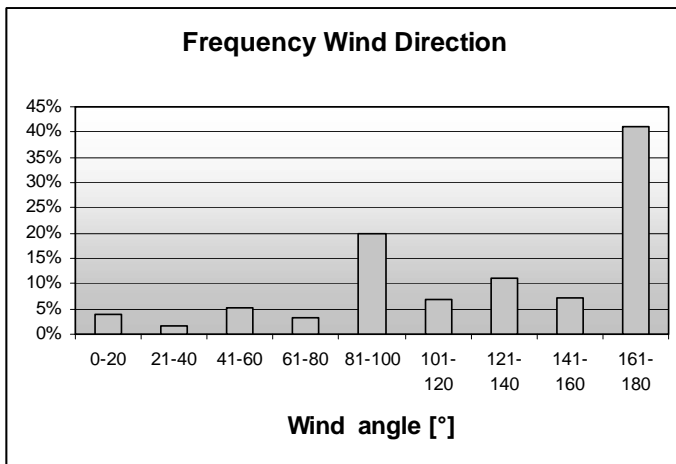
The Volvo Ocean Race

### 03 - Weather study for VPP input

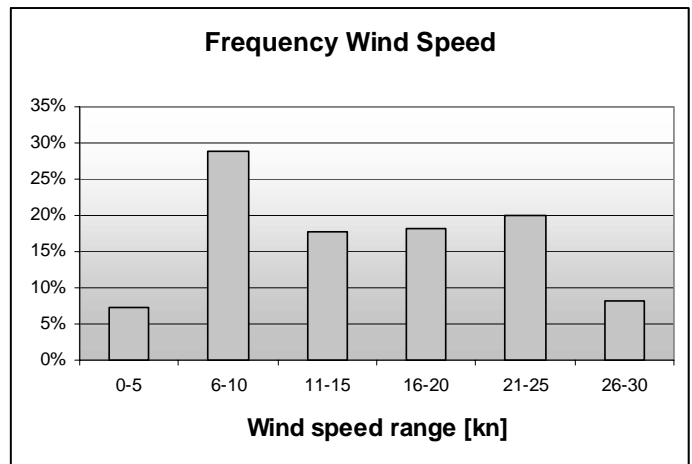
The weather study will be used to class the boats, and so is an important part. Due to cost constraints, a weather study using routing software similar to Maxsea or Raymarine Sail Racer hasn't been possible. A Vpp and a Routing software linked together is the way to go to analyse such data. The way followed was to use "grib" files (\*.grb) downloaded from internet [3] and a freeware [4] to plot the files. The grib files represents wind strength and direction prediction for the whole world. Several files were used to represent the correct time in the year for each legs. With the software, wind condition and courses could be modelled to give the weather input. The total amount of sets of wind angle/wind speed was 90 for the whole race, to enable a good accuracy. The data was then input into a Race Modeller Program (R.M.P) written in Excel, which with the speed polars from WinVPP was able to define finishing time for each leg. Such program saves a fair amount of time.

The details of the wind speeds and wind angle for each leg are shown in the appendices. (Page A1)

The two following graphs (3.a & 3.b) show the wind direction and speed frequency (time) around the world. As expected for such offshore race, running is the most important part. Light wind performance is important too.



Graph 3.a



Graph 3.b

## 04 - Weight and centres estimate

### 04.1 Introduction

A precise weight estimate is crucial in such boats where total weight is restricted, every weight saved is put in the bulb. As seen during the last Volvo ocean race, huge amount of time and money is spent on design and construction refinements. At design time, a correct weight estimate enables to have good estimate in righting moment, which is the basis of the whole design process, from performance evaluation to structural design. The difficulty is as boat beam increases, hull area increases, righting moment increases, loads increase and for example mast weight increases. This process is infinite and time need to be spent to investigate and know the influence of each item. For this project, structural weight, keel weight mast weight have been regressed against righting moment, beam, etc... to be able at the design time to access the exact weight of the boat, in other terms to be more precise. The weight estimate spreadsheets contained approximately 200 items. A margin of 5% on every item was added to take into account uncertainties. A summary of the spreadsheet is shown in the appendices (page A2).

### 04.2 Influence of beam on structural weight

The main influence of beam increase is the increase in surface area. To investigate the influence of beam on the structural weight, 3 hulls with beam of 4.7, 5.2 and 5.7 were modelled and structured using the ABS. The use of a good surface modeller and a spreadsheet made this choice a quick process. The data was then regressed to a 2<sup>nd</sup> order polynomial using best square technique;

$$\text{Structural weight} = 19.15 \cdot \text{BOA}^2 + 54.58 \cdot \text{BOA} + 1797.3$$

### 04.3 Influence of beam on rig weight

The influence of increase in beam on rig weight comes from the increase in righting moment. The VOR70 rule requires a minimum weight for the complete mast. This minimum weight is achievable over the whole range of RM by varying rig geometry (increase chainplate width for higher RM). Therefore rig weight has been found to be non dependent on beam.

## 04.4 Influence of bulb weight on fin weight

To stay at the same displacement, structural gain will be put back in the bulb. Keel fin weight varies with bulb weight. Using a similar method as explained for the hull weight, a fin weight was found to obey:

$$\text{Fin weight} = 1300 + (\text{Bulb weight} - 4500)/5$$

## 04.5 Choices affecting weight estimate

The two equations above are the one that will influence the weight by the biggest amount if the beam and/or displacement is changed. Other factor could have been included, but it would have been far more time consuming for minor changes in weight at the end.

An all-male crew was chosen it is to nine. This is the most obvious choice for the teams.

## 05 - Hull design

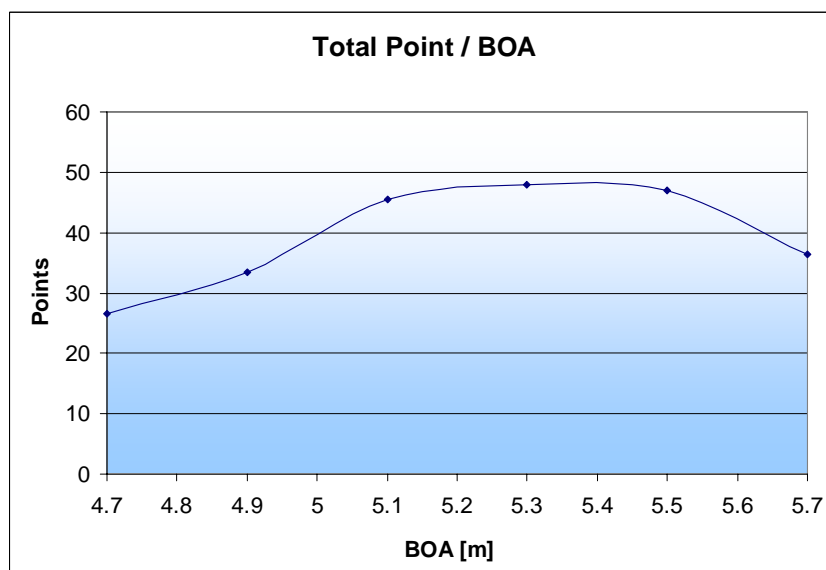
See Drawing VO70-LP1

### 05.1 Introduction

Waterline length  $L_{WL}$  has to be to the maximum, for the same displacement increasing length decreases resistance. Speed is proportional to resistance. Displacement and waterline length are the 2 main parameters affecting hull performance. The waterline beam  $B_{wl}$  (linked to canoe body draft  $T_C$  by the displacement) need to be investigated as increases in  $B_{wl}$  increases resistance at low speed and in waves but increase righting power hence power. Several geometric parameters characterise the volume distribution of a hull;  $C_p$ , LCB and LCF are the ones frequently used in yacht design. These parameters have been the subject of many researches, studying their influence on hull resistance. Delft series algorithms are results from such researches.

### 05.2 Preliminary Hull design – $B_{wl}$ iterations in $V_{pp}$

This first analysis was done to have a general view of the problem, is a thin hull as seen on CBTF is favoured over large Open hulls? Six hulls have been designed to the same displacement with different waterline beam but same  $C_p$ ,  $L_{cb}$ . Hull weight was taken the same for the 6 hulls. As seen later this assumption as a big effect on the results.



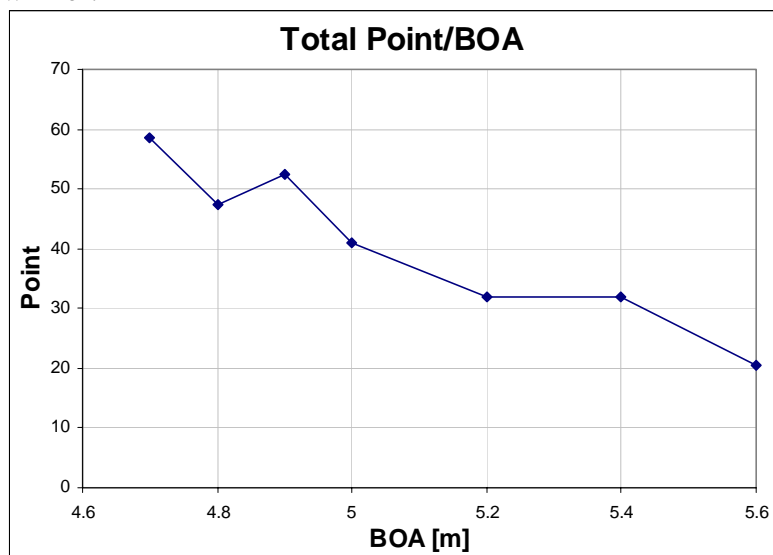
Graph 05.a: Results of hull investigation n°1. Boat points at the end of the race. More points wins.

The Vpp analysis with the weather study enables to study the influence of the changes on the whole course. As shown above there is definitely a “best range” (5.2 to 5.5m wide). This is where the design should be and it will be investigated in a more precise level.

The second step was to refine the models and include the fact that a wider hull has a higher structural weight.

### 05.3 Systematic series: Beam investigation

Using rules for scaling weights of structure, appendages, etc (as explained in *Chapter 4*) a series was designed to investigate influence of beam on performance. Six hulls with the same full displacement were designed; same full displacement means that the slimmer hull has a bigger bulb hence a smaller hull volume. Such series can be very time consuming because an important number of parameters are involved. With the aid of programming and software knowledge the time has been reduced to a maximum. (A 6 series hull with computer modelling, Vpp runs, data analysis has been done in 1 hour). A good indication of the value of using the race scoring for analysing the results is the fact that the hull with beam overall ( $B_{OA}$ ) of 4.9m has an average speed higher around the world but applying the coefficient for the legs gives the boat with  $B_{OA}$  of 4.7 as the winner.



The advantage of the slimmer design was easily seen in the 4 last legs, where it won all the legs. It is explained by the importance of light wind performance, where resistance takes over stability.

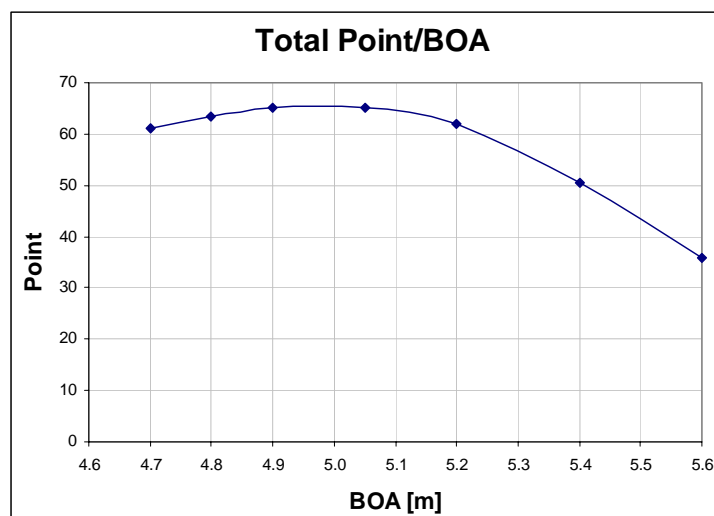
Graph 05.b – WinVPP3 beam investigation results.

It is seen that, as thought, bulb weight is very important; on a conventional boat the bulb works at a lever of  $T \sin(\text{heel})$  and a canting keel boat at a lever  $T \sin(\text{heel} + \text{cant.angle})$ , for an heel angle of  $20^\circ$  and a canting angle of  $40^\circ$  the lever is increased by 253%. A bulb will be more efficient as a producer of stability on a canting keel boat than a conventional boat. It is then obvious the proportion ballast stability/form stability must be higher for a canting keel boat than a conventionally ballasted boat. Next it was tried to go for max displacement so to put the maximum weight in the bulb. It was rewarding to do so.

The choice was for minimum beam and maximum displacement.

#### 1st series: Beam investigation with new Vpp (WinVPP4)

Results from the first investigation were seen with suspicion because the VPP was not designed to model canting keel (righting arm at  $0^\circ$  heel). Results were similar to expected but they needed to be checked, the new version of the Wolfson VPP (vers. 4) is able to model canting keel and was used to run the beam investigation. The main difference is that the predicted heel angles are higher than the 1<sup>st</sup> series, the first VPP gave heel angle limited to below  $16^\circ$  which looked strange. With the new Vpp, heel angle looks more reliable. These more important heel angle increases the influence of form stability on performance. Hence when boat displacement is fixed to the minimum, the best boat is the one with a BOA of 5.0.(results shown in Graph 05.c) But with the displacement increased to the maximum the best hull is again the thinnest one. The advantage is significant, since it corresponds to a difference of 20 hours on a round the world race. (Less than 1%).



Graph 05.c - WinVPP4 beam investigation results.

## 05.4 Midship section

The main idea in midship section design is to go for flair or not. Increase it will increase beam overall hence increase efficiency of the weights (crew + sails) situated at the edge of the deck. But as the boat heels the hull will have asymmetric waterlines therefore increase heel drag. Hull weight will be increasing at the same time. (More hull area). Vpp modelling of heel drag is not accurate enough to investigate the influence of flare on the performance of the boat. The only parameters that influence resistance of heel in the Vpp are  $B_{OA}/B_{WL}$ ,  $B_{WL}/T_C$  (upright parameters) and heeled wetted area.

### 05.4.1 Shearline, freeboards

Minimum freeboards give minimum hull weight. The rule requires minimum freeboards at the bow, stern and midship. For weight reasons, the freeboards will be to the minimum.

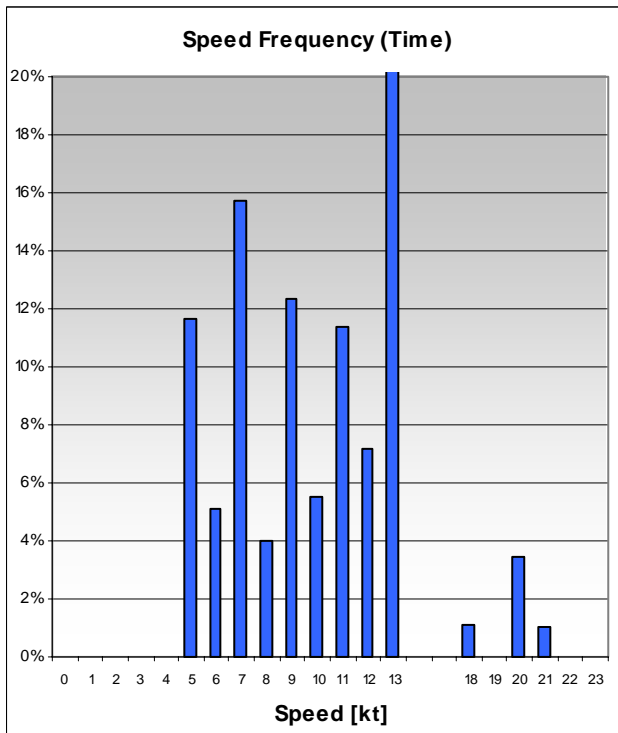
Shearline is limited too, it need to be convex with a minimum radius of curvature. The design would have used a concave shearline more conveniently, more headroom in the middle for accommodation, lower weight at bow and stern (smaller gyradius), better structural inertia to counteract rig tension, etc... The concave shearline rule is often followed by the RORC (in IRM too) and the author does not see the reasons behind this fact.

### 05.4.2 Small angle Stability issue

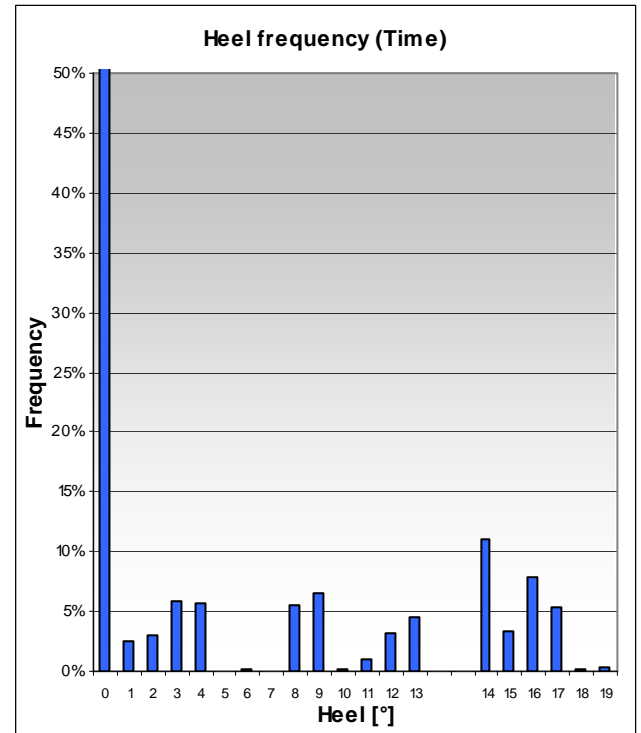
One of the most acclaimed parts of the rule is the absence of a maximum heel angle when the keel is fully canted. This has been the reason why open 60 are so wide, they need maximum initial stability. The rule influence on hull design has been checked early on, and does not influence hull design.

## 05.5 Hull design for specific speeds and heel

An area where resistance algorithms aren't as reliable as other is heel resistance. Heel resistance is a function of upright resistance, heeled wetted area, and upright LCB and  $B_{WL}/T_C$  ratio. As seen on the I.M.S. circuit, flaws exist. It has been thought more reliable to design the hull following the data that the speeds and heel angle that the speed and heel frequency graph gives us.



Graph 05.d



Graph 05.e

From the graph 05.d and 05.e it can be seen that 2 main speeds/group of speed and 2 heel angle/group of heel angle regimes are dominant; 7 and 13 knots, 0 and 14° of heel. This 2x2 matrix can be reduced to 3 states because a speed of 7 knots with 14° of heel will be rare. The “game” here is to minimize upright resistance (reduce  $B_{WL}$ ), but at the same time make sure that heeled waterline are straight and with limited wetted area. Here the influence of  $B_{WL}$  on stability hence performance is not accessed due to the fact that as seen before form stability is not of the most importance.

### 05.5.1 Optimisation of $C_p$ and LCB

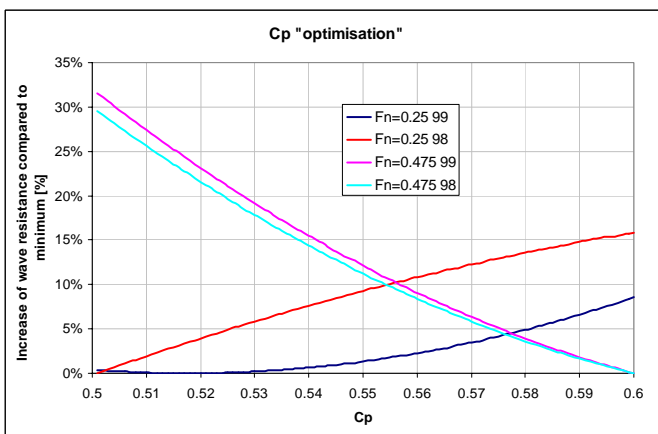
A common source for LCB and  $C_p$  optimisation is the Delft Systematic Yacht Hull Series (DSHYS) tested at the Delft University of Technology (DUT). It has been tested over the last 25 last years, constantly updating their model to reflect the current

state of yacht design. Varying a parameter each time enabled to see the influence hence an optimum.

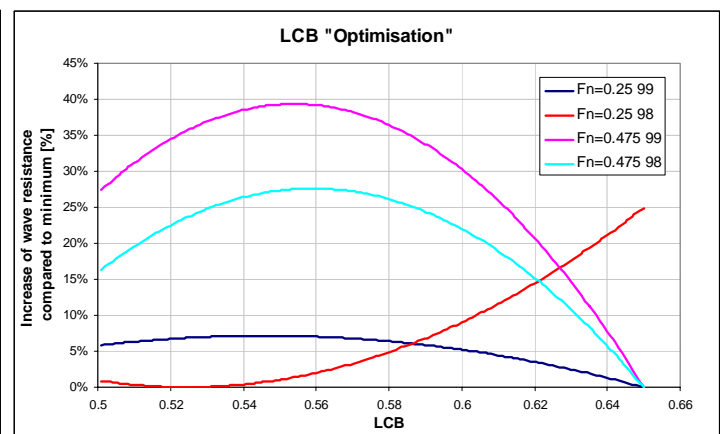
Two main algorithm were published the first in 1993 [5] and the second in 1999[6].

### “Optimum” Cp and LCB

The delft series can be used to have an idea of a good Cp and LCB, however these optimisation are done changing a parameter only and it will probably be impossible in real design for example to change Cp without affecting WSA or LCB. The results must be taken with care. The results shown below are for a certain type of boat, the optimisation using the delft algorithms are heavily influenced by the  $L_{WL}/Vol^{1/3}$  ratio, the Volvo open 70 is situated on the very top side of this ratio.



Graph 05.f



Graph 05.g

On the above graph (05.f and 05.g), only the wave resistance is used.

Another Delft algorithm has been added, it was published in 98, and is very similar to the one published in 99. The 93 algorithm is not shown on the graph because it is not possible to “optimize” either parameter for such high  $L_{WL}/Vol^{1/3}$ . With the 93 algorithm, the value of increase in drag actually grow rapidly as Cp or LCB is changed from the minimum value, it shows that the algorithm is not suited for high  $L_{WL}/Vol^{1/3}$ . Both algorithms agrees well for the higher speed ( $F_N=0.475$ ), they both agree that the ‘best’ LCB and CP are the highest value. However for the lowest speed value ( $F_N=0.25$ ), the 98 algorithm “requires” the lowest Cp and a LCB of 0.525, the 98 algorithm “requires” a Cp of 0.517 and the highest LCB.

For the upright sailing, the two speeds (7 and 13 knots) require a compromise to be done because the requirements between these two modes of sailing are different. Drag increase due to a low Cp at the highest speed is very costly, at low speed the

percentage is lower and the amount of wave drag compared to total drag is lower than at high speed, therefore a 0.54 was chosen. The aft ballast tank will be full at the highest speed and will therefore increase  $C_P$  (by trimming the boat by the stern), using a stability program it was seen that the aft tank could increase  $C_P$  up to 0.59. The increase in displacement due to the weight of the ballast tank will probably be offset by the more optimum  $C_P$  and a higher bow over the water. The aft ballast tank will have a similar effect on LCB, therefore it can be chosen quite low for  $F_N=0.25$ , a LCB of 0.53 was found reasonable. .

For the third state of optimization (Heeled + 13 kt of boat speed), the best can be more easily found. A higher  $C_P$  (0.56) can be used to accommodate the higher speed. LCB optimization is difficult here, since trim of the vessel needs also to be taken into account. Improvement of the performance with changing LCB is limited.

This “optimisation” is not only a mathematical process using a regression formulae, there is physical explanation; at low  $F_N$ , where viscous pressure drag is important, the adverse pressure gradient on the afterbody should be minimised, i.e. a forward LCB and a moderate  $C_P$  is looked for. At higher  $F_N$ , a blunter stern is desirable to delay separation and obtain a greater wave length, therefore an aft LCB and a higher  $C_P$  is required.

The use of the aft ballast tank in high speed case has the role of moving LCB aft and therefore increasing wave length, its second role is to increase trim and reduce pitch poling probability.

From these 3 modes of sailing, using a geometry modeller, the hull was designed for a  $C_P$  of 0.54 upright and a  $C_P$  of 0.56 at 14° of heel, then a compromise between waterline asymmetry and wetted area heeled and upright was achieved. The trimming moment from the sail was incorporated to take into account the change of shape, due to the fact that the crew weight is not important enough to trim the boat.

### 05.5.2 Assumptions of the method, problems

The DSYHS have been done upright for zero yaw and zero leeway. Leeway and heel as well produce dissymmetry of the pressure along the hull which affects wave resistance. These factors will affect the capability of the algorithms, but it is still found to be a reasonable approximation.

Volvo 70 are a different breed of boat, technology advance have given possible to reduce displacement by large amount. Length displacement ratios are the most

influential parameters on hull resistance and behaviour. Care is to be taken here, because a Volvo 70 hull is just over the limit where Delft studies are applicable, two ratios are above the tested matrix; the slenderness ratio ( $L_{WL}/Vol^{1/3}$ ) is 8.6 and the Delft limit is 8.5, and the Length/Beam ratio is 5.81 compared to the limit of 5. As seen in the literature and this project the Delft series look to approximate very well the resistance even out of the limit of the matrix.

## 05.6 Towing tank input

Wave generated by the hull seemed very small; this is due to the big  $L_{WL}/Disp$  ratio and moderate  $L_{WL}/B_{WL}$ . A strange observation was the generation of the bow wave, the forward waterlines are very thin and they were apparently two bow waves. It was thought that the bow waterlines were too thin so the forward waterlines on the final design were made wider. This has also the effect of reducing trimming angle when heeled.

The hull was finally faired using common surface curvature tools (Gaussian & Normal 0-90°).

## 05.7 Conclusion

The hull has been designed using VPP as the main tool. The procedure followed has enabled the design of the best hull in the limit of the parameters and limitations taken. One of the most important is the weather model employed.

The study shows the benefice to go for a low resistance hull. This conclusion is different from what is seen in the Open 60 fleet, the difference is mainly in the rule. The open 60 rule states that at rest with keel fully canted the boats should not heel more than 10°, therefore a wide enables to use large keel angle. Such rule doesn't exist in the VOR70; the VOR70 should actually heel up to 24° with the keel canted to 40°.

*The hydrostatic table are shown in the appendices. (Page A3)*

## 06 - VPP configuration

The following states what and how VPPs was used and configured.

### 06.1 VPP 3.X

The first VPP used was the Wolfson Unit WinVPP version 3. It doesn't model canting keel, but using a transverse shift of the centre of gravity to model the canting keel, good results were found reasonable. The Vpp didn't model the loss of side force due to the cant angle. It was thought that these factors do not affect the results for beam variation.

### 06.2 VPP 4.X

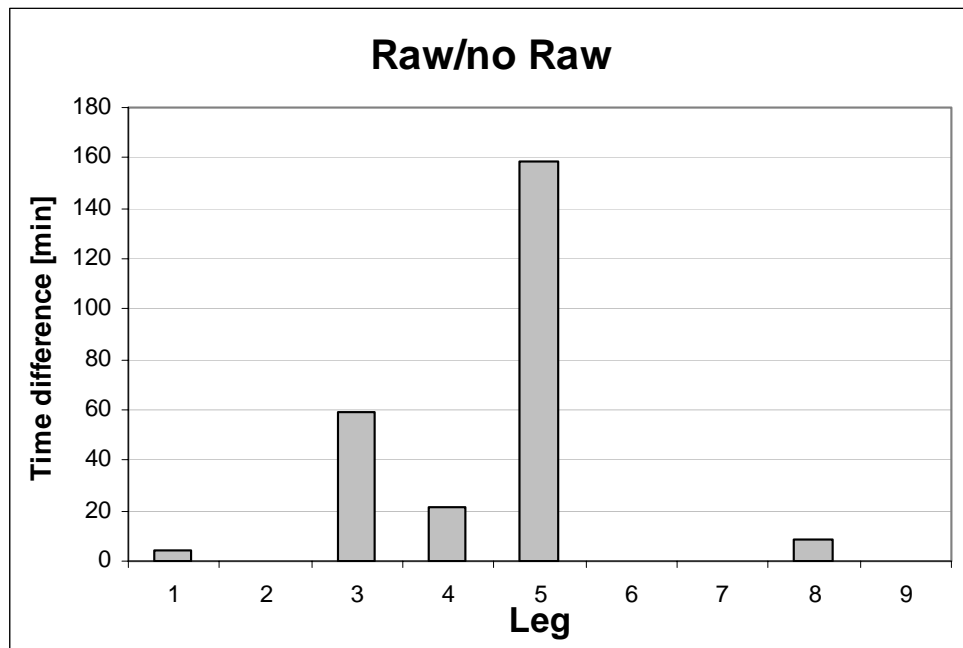
As soon as it was available, the Wolfson Unit WinVPP 4 was used. This new version is able to model canting keels and many kinds of appendages configuration. However it probably lacked beta testing or similar, because the version was found more unstable than the previous version both for non-canting and canting cases. Moreover this version models many appendages configuration. It is not known exactly how they are modelled; therefore it is difficult to make any definitive conclusions.

### 06.3 Common file

The general file run in the VPP consists of 2 flotations (canted and not) and a same rig with, one mainsail, one jib, one Solent, one inter a masthead spinnaker and a fractional spinnaker. It gave 5 "opsets". A common run time was around 5 seconds.

### 06.4 Resistance added in waves (RAW)

A resistance added in waves has been added to take into account that a wider beam gives bigger added resistance in waves than a small beam. Graph 6.a shows the influence of taking into account this added resistance on the time to finish the legs. The influence is small and won't make a big difference.



Graph 6.a: Legs time difference if added resistance in wave is used.

## 07 - Appendages design

### 07.1 Introduction

The main purpose of the appendages is to control and balance the forces and moments generated by the sails. The objective in advanced yacht development is to design appendages which perform these tasks as efficiently as possible; produce minimum resistance for a given amount of hydrodynamic lift. The two main drag parts are induced drag (or vortex drag) and viscous drag (skin friction + pressure drag).

Induced drag is present only on finite span wings, it is due to pressure difference at the tip, it produces spanwise flow which rolls up in vortex sheet at the trailing edge. Induced drag coefficient is inversely proportional to aspect ratio ( $\text{Span}^2/\text{area}$ ). On a conventional fin keel yacht induced drag is around 10% of total drag upwind.

Viscous drag is mainly determined by the state of the boundary layer (laminar, transitional, turbulent, or separated) over its surface. Flow separation at the trailing edge results in negative static pressure at that location which produces pressure drag.

The main restriction imposed by the rule is that each appendage can only have one degree of freedom (rotation, retraction, etc.). For example in case of the CBTF, the forward rudder can't be lifted off, or in the daggerboard case, their angle of attack cannot be changed. It also states that "No appendage shall have an angle relative to the longitudinal centre plane of greater than 30 degrees, measured between any two points in a plane parallel to the maximum thickness." This removes the possibility of adding winglets on the bulb for example.

Towing tank testing has been done before finalising appendages design, after analysing the towing tank results (*see chapter 8 and 9*). It was found that a CBTF configuration would be faster over the Volvo Ocean race, therefore the following parts deals with the design of such appendages.

Trim tab, as seen on powerboats, are allowed by the rule. Such appendages should give similar potential as seen on powerboats. But unfortunately there was not enough time and resources to investigate this interesting subject in a deeper way.

## 07.2 Bulb design

*See plan VO70-A1*

### 07.2.1 Overview

The requirement of the canting keel is to carry the bulb; very limited sideforce will be produced by the keel. As such the bulb has no requirement to act as an endplate to reduce tip vortex ;( i.e. induced drag). Bulb optimisation is to reduce drag and lower the centre of gravity; such study can be done without thinking about the fin.

### 07.2.2 Computational Fluid Dynamic

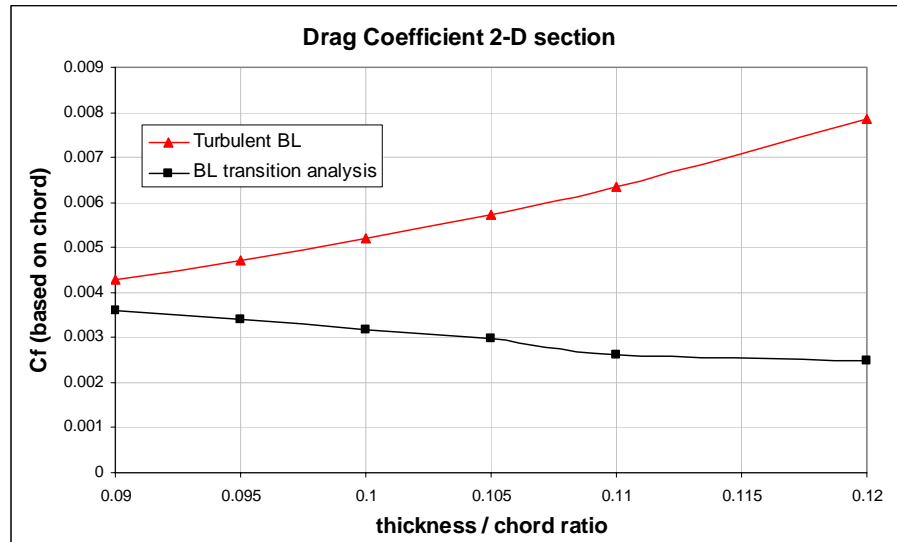
A CFD RANSE study of bulb shapes was not found time-efficient and result-efficient due to several reasons.

As seen during the last America's cup, bulb design is still a very open part and not well understood part of yacht design. This can be explained by the difficulty to predict the behaviour of the boundary layer (transition and separation) over such 3d body, and the limited investigation done by aeronautic company on similar bodies. Not much technical papers have been done on such bodies, except tip tanks and underwater missile. They most often deal with completely turbulent flow and no angle of attack. Optimum body geometry can be found for complete turbulent flow. But large gain can be getting in increasing the laminar extent on the body. This lack of knowledge can be shown looking at the bulb design process of the winner of the last America's cup Alinghi; they assumed laminar boundary layer flow over a finite length from experimental work. There is also lack of knowledge of turbulence behaviour differences between water and air.

Using today Turbulence algorithm in the design of bulb can give wrong results. It is common knowledge that RANSE solver will give the advantage to longer bulb.

#### **Example**

A good example of the problem can be shown with a study of the best thickness chord ratio for a 2d foil. The next graph (*Graph 07.2.a*) shows the results of the analysis using two different configuration, the first one the one assuming the boundary layer to be completely



Graph 07.2.a

turbulent (as in RANSE), the second is where transition is modelled using the  $e^N$  method. This analysis represents a bulb cross section, therefore the cross section revolved around its axis must have the same volume, and an increase in  $t/c$  ratio gives a decrease in length hence in Reynolds number. The graph clearly shows that the conclusion are opposite, increasing  $t/c$  in the turbulent case increases area (wetted length/chord is higher) and pressure drag is increased, and therefore increases overall drag. In the case where laminar to turbulent transition is modelled, increasing  $t/c$  decreases drag, it is due to the fact that as  $t/c$  increases, pressure gradient on the fore body increases and therefore laminar flow can be sustained for a longer length.

### 07.2.3 Preliminary Bulb shape

#### 07.2.3.1 Assumptions, main aspects

To study bulb drag, it is important to deal with angle of attack; as shown next the flow on a revolved body at an angle  $\alpha$  to the flow has streamlines over its body of  $2 \cdot \alpha$  (Diagram 07.2.a). However leeway or pitch angle on such boats will be assumed to be small enough to be neglected.

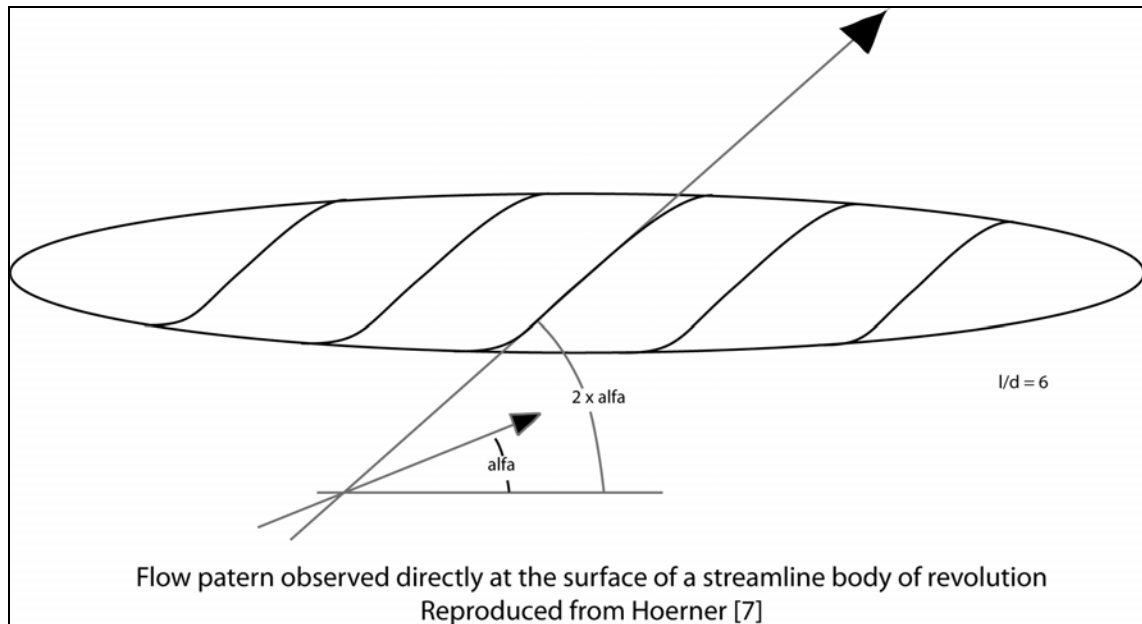


Diagram 07.2.a

The difficulty is the value of Reynolds number (around  $5e6$ ) which put us in the middle of transitional range (between laminar and turbulent). This is where large gain can be made. Decrease in drag as much as 50% can be achieved. These high decreases are achievable with body designed for specific  $R_n$  and with high  $D/L$  which is not applicable to the main role of the bulb; produce righting moment deep down. Drag predictions are problematic, however, as transition is difficult to predict.

Laminar flow on the forward part requires good pressure gradients hence a maximum thickness at the back and an important  $D/L$ .

Another area of research is to make the bulb asymmetric in the horizontal plane to move its cog down. Such aspect has to be thought through due to the fact that the bulb will produce lift (directed upward) and be a nuisance when the keel is canted. It will increase base drag too.

Bulb has different requirement that affects its design, they are lower the CoG, act as an endplate, and limit its resistance. In fixed keel yacht a complex compromise has to be found, as shown is the last America's cup the choices are difficult. A canting keel boat has the advantage that the keel is not the main source of lift hence the bulb doesn't have to be optimised to be effective as endplate.

The importance of placing the CoG of the bulb deep down is expected to be an important factor, on fixed keel yacht a 1cm gain in CoG will give a gain of  $1 \cdot \sin(\text{heel})$  of righting moment (righting moment can be expected to be proportional to GM for narrow boats). On a canting keel yacht a 1cm gain in CoG will give a gain of

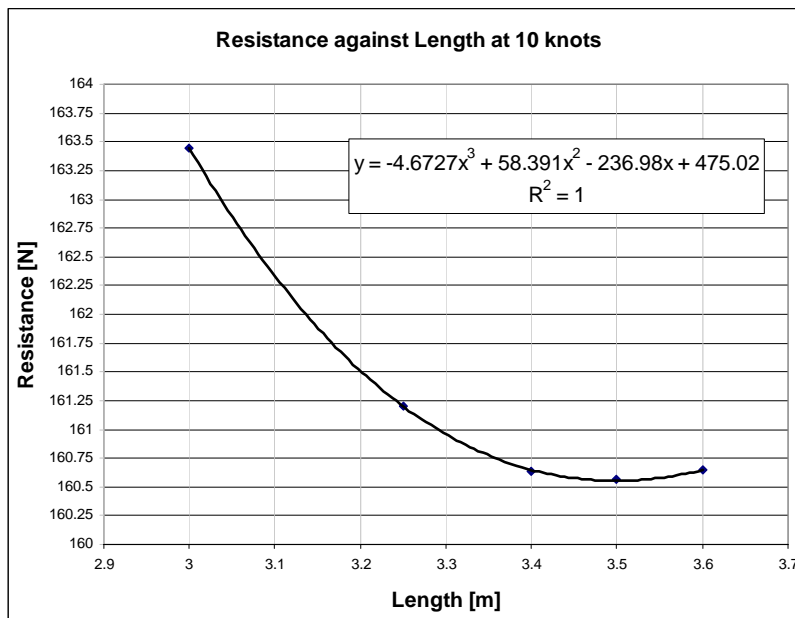
$l \cdot \sin(\text{heel} + \text{CKangle})$  of righting moment; for a heel angle of 15 the gain in RM is higher by 316 %.

### 07.2.3.2 Length

The design process is started using statistical regression data of streamline rotationally symmetric bodies. Such data can be found in Hoerner [8], above the critical Reynolds number (around  $10^5$ ), an interpolation of the data point is found to give a total drag based on wetted area of:

$$C_D = C_F \cdot (1 + 1.5 (d_B/l_B)^{3/2} + 7(d_B/l_B)^3) \quad \text{eq.7.2.1}$$

Where  $1.5 (d_B/l_B)^{3/2}$  is the average increment in dynamic pressure along the sides (super-velocity), and  $7(d_B/l_B)^3$  the drag component due to flow separation.  $d_B/l_B$  is



the diameter length ratio. Bulb  $l_B/d_B$  could be optimised quickly using the formula above, but  $C_F$  is related to  $l_B$  as well (increasing  $R_N$  reduces  $C_F$  at high  $R_N$ ). Therefore the optimum length for lower drag in symmetric flow is calculated by

designing a series of bulb of the same volume, and measuring area, length and diameter. Such process gave the following graph where an optimum can be seen at a  $l_B = 3.51$  m. The next step was to optimise the cross section.

### 07.2.3.3 Cross section shape

Cross section shape has two main influence on bulb performance, (for now the approach will be limited to elliptic shapes), firstly changing the cross section from a circle to an ellipse will increase wetted area, therefore drag will increase, secondly as height/beam ratio is increased,  $VCG_{\text{BULB}}$  gets deeper therefore GZ increases, hence performance increases. This is another case where the Vpp is the tool that will enables the choices to be made.

### 07.2.3.3.1 Relation Centre of gravity – Increase of drag bulb (VPP study)

A VPP study was required to see the relation between changing the bulb shape to deepen the centre of gravity of the bulb and bulb drag. In general shaping the bulb to deepen its centre of gravity will increase the drag of the bulb. Obviously it is difficult to present a definitive answer since the bulb is required to operate at angle of attack and heel.

The relation needed is: what is the resistance increase that will match the performance increase due to the bulb being deeper, this will give the “envelope” for the bulb design. To simulate an added resistance, WinVPP is not very user friendly, the only way was to use propeller to do the job. (Input using the experimental method: towing tank but was found highly inefficient). This use corresponds well since it obeys a  $qV^2$  for varying speed. The R.M.P was again used to simulate the race. The result is shown in graph 07b (pink curve). For example the increase in performance due to the bulb COG being 5 cm deeper is equal to a decrease of total resistance of 9.3N.

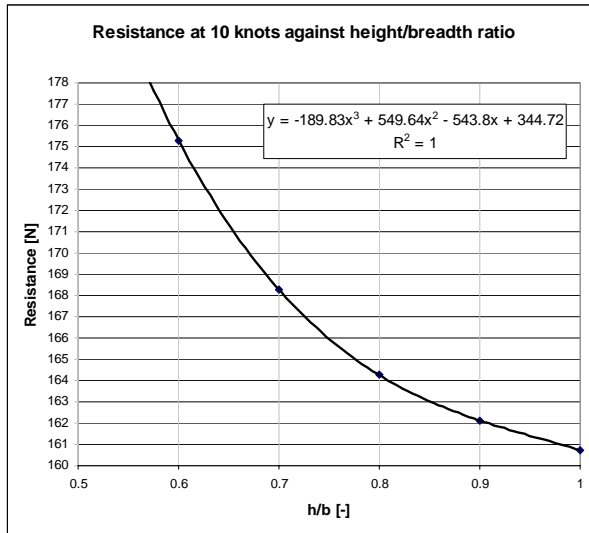
### 07.2.3.3.2 Height/Breadth ratio

Here again eq. 1 was used, the problem here is that the equation is for rotational bodies, no account is given for an elliptic cross section. A common approach is to use  $d_B/l_B$  as the average value of the sideview and topview ratios. The author does not find this approach correct since both the super-velocity term and separation term are term related to  $(d_B/l_B)^X$ , X being superior to 1. A better approach would be to average the drag.

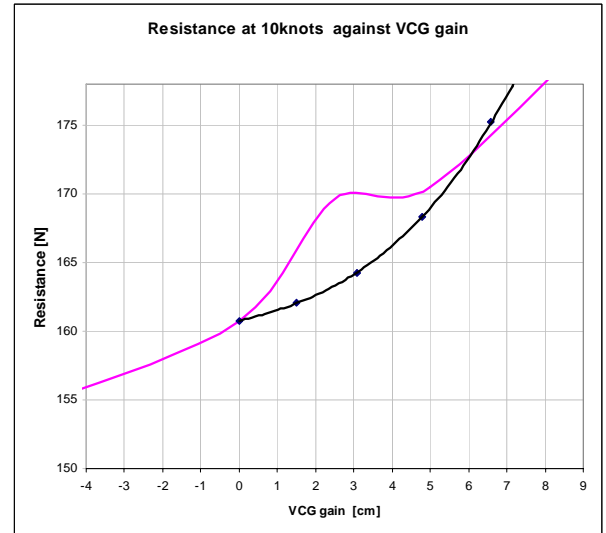
$$C_D = C_F * [(1 + 1.5 (t_T/l_T)^{3/2} + 7(t_T/l_T)^3) + (1 + 1.5 (t_S/l_S)^{3/2} + 7(t_S/l_S)^3)] / 2 \quad \text{eq. 2}$$

Where subscript T and S represents top and sideview respectively

Obviously such equation is still an approximation, but it should give good results for the preliminary design.



Graph 07.2b



Graph 07.2c

Graph 07.2b shows the resistance at 10 knots of same volume bulb where the ratio height over breadth is varied. As expected a decrease of the ratio increases the drag. Graph 07.2c uses the value from graph 07.2b to find when it is beneficial to decrease h/b. As said above the pink curve represents the limit where it is not beneficial to increase the  $VCG_{BULB}$ . It can be seen that a gain of 6 cm is still good; it represents a drag of 172.5N and going back to 07.2a, an h/b of 0.63.

Such theory assumes a fix transition point, the thickness distribution does not influence the amount of laminar flow which his not correct. A large beam to height ratio will give a flat bottom and no favourable gradient to promote laminar flow. Therefore a limit has to be put. With the influence of length and h/b more accurate, a better design of the section could be done.

#### 07.2.4 Computational tool aided design

Analogy between sphere/cylinder and bulb/airfoil section can be used to have a deeper look at bulb design. Potential flow theory states that the velocity increment (above free stream velocity) on the sphere is half that of the cylinder ( $V_{SPHERE} = V_{\infty} * 3/2 \sin \theta$ ;  $V_{CYLINDER} = V_{\infty} * 2 \sin \theta$ ). This is what is called 3D relieving effect. This relationship stays correct for the flow around a bulb (with circular cross section) and an airfoil section. It is expected that the velocity distribution (in an inviscid case: no boundary layer) around a bulb will be the same to that a foil section having half the thickness length ratio of the bulb. It can be deduced that the influence of the pressure and speed distribution on the transition point will be the same. This relieving effect will

decrease the gradients, maintenance of laminar flow will be more difficult but separation will be less likely.

However, the similarity doesn't hold for the boundary layer, on the nose, the boundary layer will expand laterally therefore will be thinner, laminar flow will be easier to maintain. In the pressure recovery, the reverse occurs; the turbulent BL will increase and might separate.

Using CFX to see the influence of the boundary layer on the pressure distribution compared to inviscid case was beneficial, it showed that in the recovery region the thickening of the BL was an important parameter. Navier Stokes solvers must run all laminar or all turbulent, so no check was done on the influence on the nose section.

The design process was to design an airfoil section that follows the above discussion and remarks. Using past experiment (see Lurie [9] and Carmichael [10]), the expansion of the boundary layer has a big influence on maintaining BL laminar. Therefore it was assumed that a laminar boundary layer could be sustained up to 60% of the bulb length with an acceptable shape. Therefore the section was designed to provide a fair favourable pressure gradient up to 60% of the chord. Then after transition a gentle recovery region was designed to take into account the fact that the boundary layer on the bulb will thicken quickly. The process is shown in diagram 07.2b

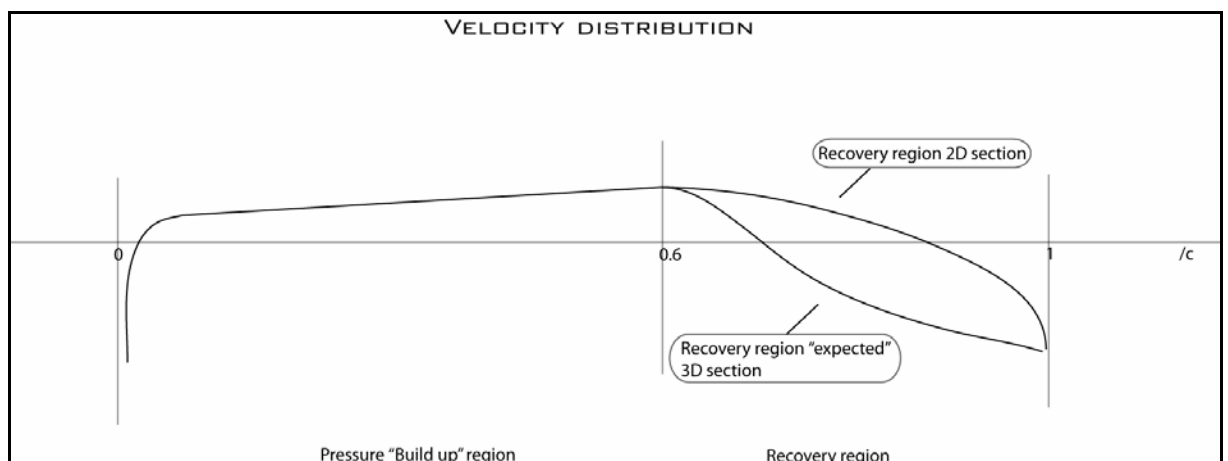


Diagram 07.2b

Pressure gradients on the 'pressure build up region' could have been made more important by decreasing nose radius, but it would cause high speeds on the nose when an important yaw angle is applied, hence a probable loss of laminar flow.

Finally the section was scaled by 2 in the thickness axis to give the bulb side-view shape. From the cross section discussion, a certain amount of elliptic cross section is beneficial (see above discussion), but transition development is not taken into account. Such theory assumes a fix transition point, the thickness distribution does not influence the amount of laminar flow which is not correct. A large beam to height ratio will give a flat bottom and no favourable gradient to promote laminar flow. Therefore a limit has to be put. The increase in laminar flow is an important factor since the decrease in drag is important. If the bottom surface is considered to be 25% of the total area a loss of laminar flow of 40% of this area will give an increase of drag of about 10%. A limit of height / breadth ratio of 0.85 was seen as reasonable.

### 07.2.5 Conclusion

For future work, it will obviously be interesting to study laminar boundary layer development using an  $e^N$  approach or similar, but the next version of CFX will have an algorithm to deal with transition. CFD RANS analysis is still very time consuming job, and therefore expensive. A 3D panel method with a method for boundary layer approach might be an interesting tool to develop since run times and therefore price will be far less.

## 07.3 Rudders

### 07.3.1 Introduction

The appendages system chosen is the one where forward and aft rudders are producing most of the required sideforce and a canting keel maximizing the righting moment.

### 07.3.2 System aspects: theory

When taking (turning), the rudders have opposite angle of attack to increase turning moment, and therefore maneuverability.

When sideforce is needed, the rudders work collectively (same angle of attack), both shares a part of the required sideforce and leeway can be reduced.

$$C_{Di} = \frac{C_L^2}{\varepsilon\pi A Re} \quad \text{eq. 07.3.a} \quad X = C_x \frac{1}{2} \rho AV^2$$

$$Di = \frac{2L^2}{\varepsilon\pi\rho V^2 b^2} \quad \text{eq. 07.3.b}$$

Therefore if the required lift (L) is the same, it can be shared by the two rudders having the same span. If there is no interference between the two surfaces, the induced drag (Di) is decreased by two fold compared to daggerboard system where the daggerboard is producing most of the sideforce. ( $2 \times (\frac{L}{2})^2 = \frac{L^2}{2}$ ).

Equation 07.3.b actually point to a misconception of many people, it shows clearly that induced drag is inversely proportional to span<sup>2</sup> and not aspect ratio. Aspect ratio is present in the coefficient form because it is non-dimensional taking planform area as basis.

### 07.3.3 System aspects: practice

#### 07.3.3.1 Main aspects

The ability of the system to shift the CLR fore and aft, to balance the hydrodynamic and aerodynamics forces is seen by the author to be of great importance.

It will probably give a new way to sail, when sailing a common way to reduce loading on the rudder is to reduce loading on the mainsail therefore decreasing drive force. Limited studies exist on the effect of longitudinal equilibrium on performance. Mainly due to the fact that a limited amount of data are available about centres of lateral resistance both for the sails and foils, and the influence of changing the sails controls. However it has to be said that if the boat is not in equilibrium when both rudders are producing the same lift which is the optimum configuration, one of the rudder will need to be unloaded and therefore L/D ratio will go down. A better way to align CLR and CE would be to move the rig CE by raking it or by tweaking it.

### 07.3.3.2 Longitudinal balance

Longitudinal balance is an important parameter for offshore racer, a balanced boat will require less adjustment by the crew to stay on course. A system with a forward and aft rudder will obviously give great benefit here; it will be able to move the centre of lateral resistance over a large length. At first, this system will obviously be harder to handle to get grips to, but in long term it has great potential.

### 07.3.4 Longitudinal position of the rudders

The position chosen on the towing tank model were generally found to be satisfying, the forward rudder interacts well with the forward wave crest, and the aft rudder root is underwater until high heel angle. The forward rudder will be moved 50 cm (full size) forward, as it thought that the interaction will be higher. The aft rudder position needs to satisfy two requirements; be well underwater at conventional heel angle, and give a CLR that will match the CE of the sails. This last statement needs to be satisfied if the performance of twin lifting devices is to be maximized, longitudinal stability need to be achieved when both rudders are producing a similar amount of lift.

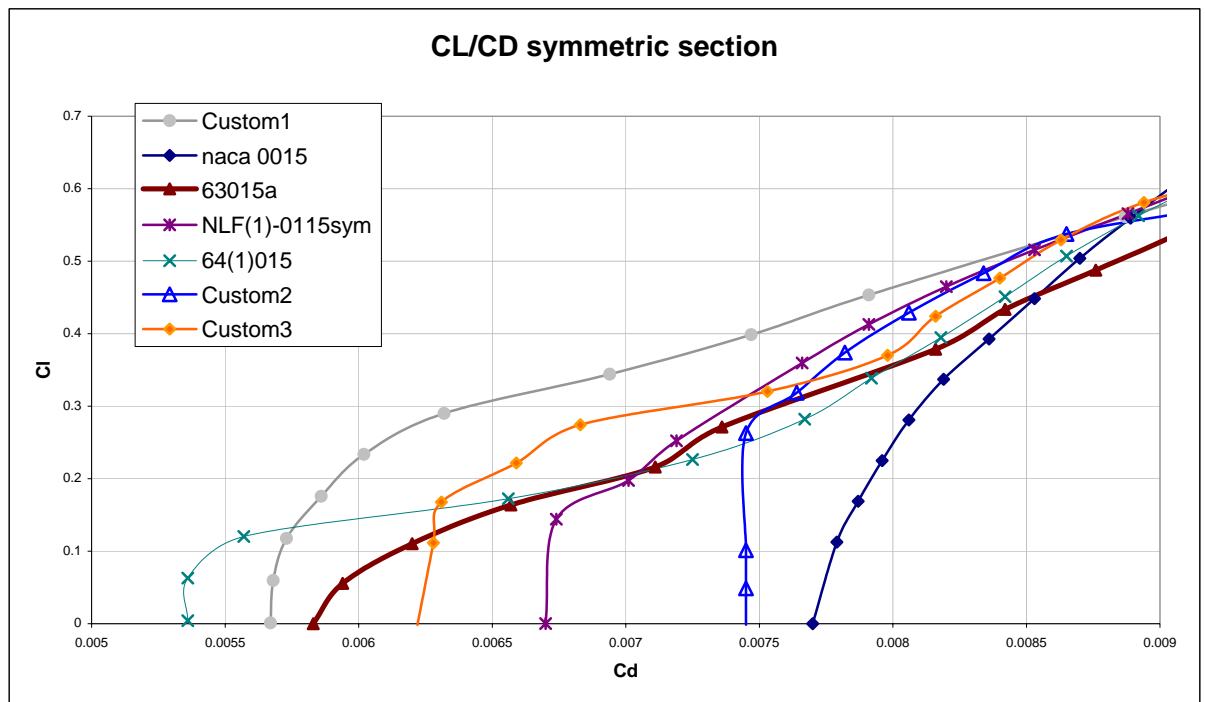
A parametric study was needed to investigate the relation between CLR and CE for such appendages configuration.

Longitudinal position of the rudders compared to the sail plan is not as important as first thought. To move the CLR 1% of LWL (20 cm), a rudder needs to produce 4% more sideforce than the other, this non-optimal sharing increases induced drag only by 0.02%. Induced drag increases to 10% when sharing is 65/35, to 20% when sharing is 72/28, so large gain can be get when lift is shared.

The final position was chosen considering other CBTF boats. Compared to other boats, the canting keel due to its drag will produce a moment directed to windward. Such influence is probably counteracted by the fact that the hull are thin and with less asymmetry, this sums to give lead values very similar to common fractional rig boats.

### 07.3.5 Rudder sections

Rudder sections need to be investigated with a 2D panel method. On such boats lift produced by the rudder is pretty small compared to racing round the buoys boats. A lot of time is spent when no sideforce is needed. Rudder sections operate at bigger angles than other appendages because they steer the boat.



Graph. 07.3.a

A comparative study was done (Graph 07.3.a) on possible sections for rudders, the program used was X-Foil (N-Crit=2). It compares common used sections (Naca) to custom designed ones. The process used to design custom section was to adopt thickness distribution of modern asymmetric section (Fx, Ls, etc..) and tweak the leading radius. The best section Custom 1 shows a wide drag bucket with very good performance up to Cl of 0.55. The section is well behaved until high Cl, and doesn't show any pressure peak (as 6-digit series) which might cause separation and ventilation.

### 07.3.6 Rudders area

For the lowest induced drag upwind both rudders should produce the same amount of lift.

Contrary to keel sizing on conventional boats, the rudders, as they are able to increase their angle of attack are not designed to stay in the drag bucket. Rudder area is dictated by the fact that the rudders need to operate in a wide range of condition, from upwind overpowered sail plan in waves, to light downwind. The first condition will require large sideforce to be produced; a too small rudder might stall. The second shows that in certain condition the rudders will need to have minimum drag.

If stall was not a problem, the rudders could operate at their best lift drag ratio which is around  $C_L$  of 1.1 for most section.

The planform needs to have a constant  $C_L$  along the span. So that  $C_L$  stall is reached at the same time on all the planform.

Something against a true elliptic planform is tip treatment. Tip shape on elliptic planform is not the best.

The VPP was again used to simulate the sailing condition and find the maximum loading the rudders will experience under normal sailing condition. The following table (Table 07.a) represents the loading ( $C_L$ ) for a single rudder assuming an area of 1.2m<sup>2</sup> and that the rudders produce 85% of the total side force.

Vt[kn]	Vb[kn]	Fh[kg]	Heel[°]	Lift[kg]	$C_L$
4.0	4.87	457.00	2.90	457.59	0.494
5.0	5.93	695.00	4.50	697.15	0.507
6.0	6.88	967.00	6.50	973.26	0.526
7.0	7.70	1265.00	9.00	1280.77	0.552
8.0	8.35	1546.00	12.40	1582.93	0.581
9.0	8.72	1620.00	13.80	1668.15	0.561
10.0	8.97	1654.00	14.50	1708.42	0.542
12.0	9.35	1736.00	15.60	1802.40	0.527
14.0	9.69	1885.00	15.90	1959.99	0.534
16.0	9.96	2027.00	16.10	2109.75	0.543
20.0	10.38	2298.00	16.60	2397.94	0.569
25.0	10.75	2624.00	17.20	2746.84	0.607
30.0	11.02	2945.00	17.70	3091.34	0.651
35.0	11.22	3268.00	18.30	3442.08	0.699

Table 07.3.a Single Rudder Loading

$C_L$  of 0.7 is reached for the highest wind speed upwind, 0.7 was chosen as the maximum  $C_L$  because it gives a “factor of safety” of 1.85 for taking, upwind in waves, etc. Such factor is following current practice in racing yacht design.

It could be argued that the rudder section chosen has a low  $C_{l_{stall}}$ , and therefore the required area is large, and that a conventional Naca 0015 which has a high  $C_{l_{stall}}$  could be better. However the decrease in wetted area will not make completely for the increase of minimum drag ( $C_{d0}$ ) downwind. And upwind the main factor is rudder span to limit induced drag, a decrease in area will provoke a decrease in chord; and since the rudder is designed using  $C_{l_{stall}} \times \text{area}$  (which is constant here), the Naca 0015 rudder wont accommodate the required rudder stock.

### 07.3.7 Rudder planform

#### 07.3.7.1 Overview: rudder interaction

The forward rudder creates a non uniform downwash which affects the aft rudder. Munk in [11] shows that the induced drag is a minimum when the downwash is constant, for an isolated planar wing in a uniform flow a elliptic planform will produce this constant downwash. However for the aft rudder which is operating in the downwash of the forward rudder, an elliptic planform won't give a constant downwash across the span.

It was then required to get the downwash distribution at the aft rudder.

#### 07.3.7.2 Forward rudder

The structural design of the rudder stock plays an important part here; the required section of the stock with a specified t/c ratio for the rudder foot gives the rudder root chord. It was found that a root t/c of 0.16 was achievable with a chord of 0.596 m, using a planform similar to a parabola it gives a span of 3.014 m. Having in mind that the rudder stock will require an angle of  $3^\circ$  forward to stay normal to the hull, and that it needs to feat into the rudder, the planform started with a straight trailing edge and a semi-parabola leading edge, then to have a straighter quarter chord line and to make space for the stock, the trailing edge was angled forward and changed to an arc. The tip was then chopped off to enable a better tip (squarer). The parabolic chord distribution has several advantages here, it increases lift slope, and decreases induced drag, and gives a constant Cl distribution across the span. Therefore  $C_{L_{stall}}$  of the rudder will be similar to  $C_{l_{stall}}$  of the section.

### 07.3.7.3 Aft rudder

#### 07.3.7.3.1 Introduction

Lifting line theory can be used to investigate 3d effect on upswept and high aspect ratio wing. The equation for induced drag of an elliptic lift distribution is well known (eq. 07.3.1 with  $\varepsilon=0$ ) comes from such theory. The same theory can be used to investigate the influence of a non elliptic distribution. The aft rudder will operate in the downwash of the forward rudder; to investigate its influence an extended lifting line program can be used.

#### 07.3.7.3.2 Lifting line

The wing circulation is modeled as a bound vortex system located at the 1/4 chord position and with its associated shed vortex sheet (diagram 07.3.a). The spanwise circulation distribution (or bound vortex strength distribution) is represented by a Fourier sine series consisting of N terms:

$$\Gamma(\phi) = 4sU_{\infty} \sum_1^n A_n \sin n\phi$$

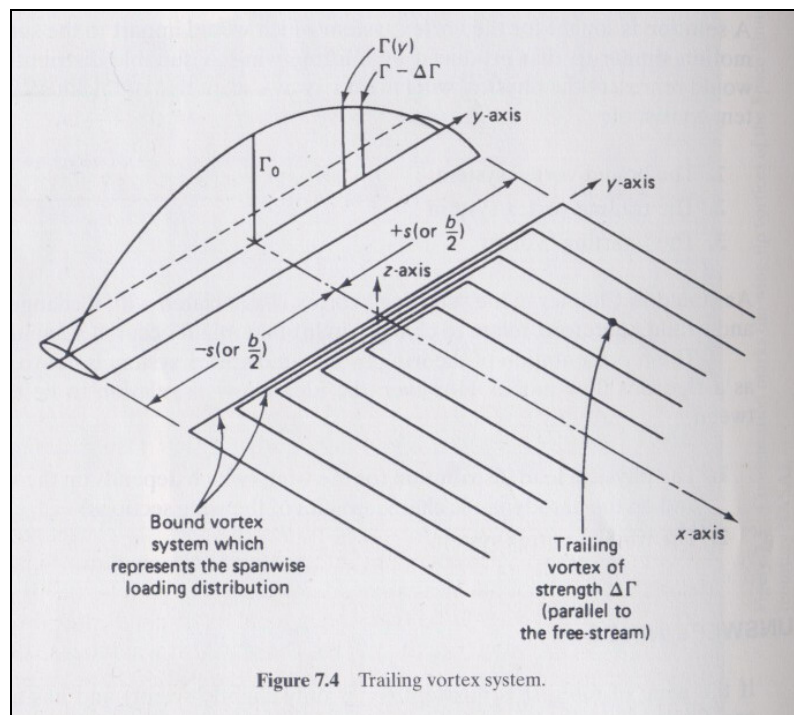


Diagram 07.3.a from [12]

The spanwise distribution is modeled by a finite number of bound vortex associated by its two shed semi infinite vortices, this forms a horseshoe vortex. It is required to evaluate such system using numerical techniques, a program was therefore written. When the wing analysis is finished, the horseshoe vortices strengths are known and therefore downwash can be calculated. Biot-Savart law states the cumulative effect of all trailing vortices induces a velocity  $W_{y1}$  at a point  $y_1$ ,

$$w_{y1} = \frac{1}{4\pi} \int_{-s}^{+s} \frac{d\Gamma / dy}{y - y1} dy \quad \text{eq. 07.3.c}$$

This downwash will be constant along the x axis because the expression has no variable changing with x.

The influence of the bound vortex is more straightforward, since it is a finite length vortex filament and it will be all the time upwind of the area under investigation.

$$w_{y1} = \frac{\Gamma}{4\pi} \int_{s_1}^{s_2} \frac{\sin \alpha}{a^2} ds \quad \text{eq. 07.3.d}$$

$$w_{y1} = \frac{\Gamma}{4\pi R} (\cos \alpha_1 + \cos \alpha_2) \quad \text{eq. 07.3.e}$$

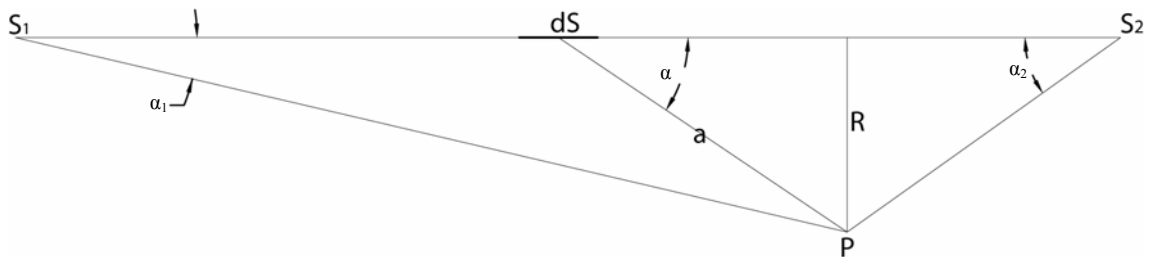
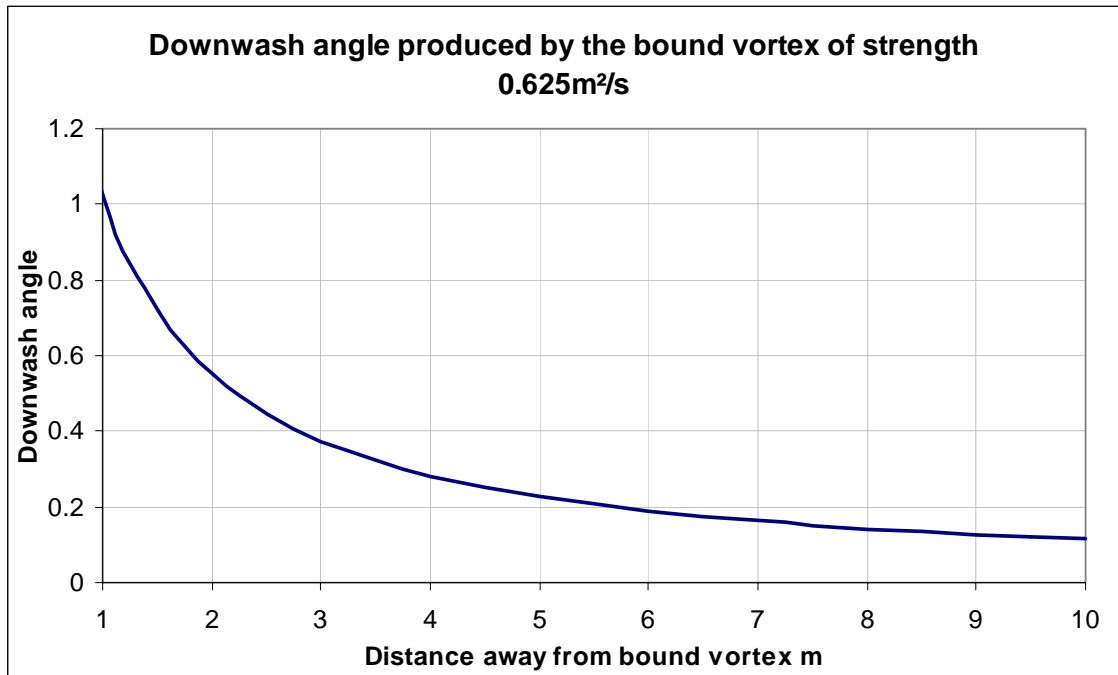


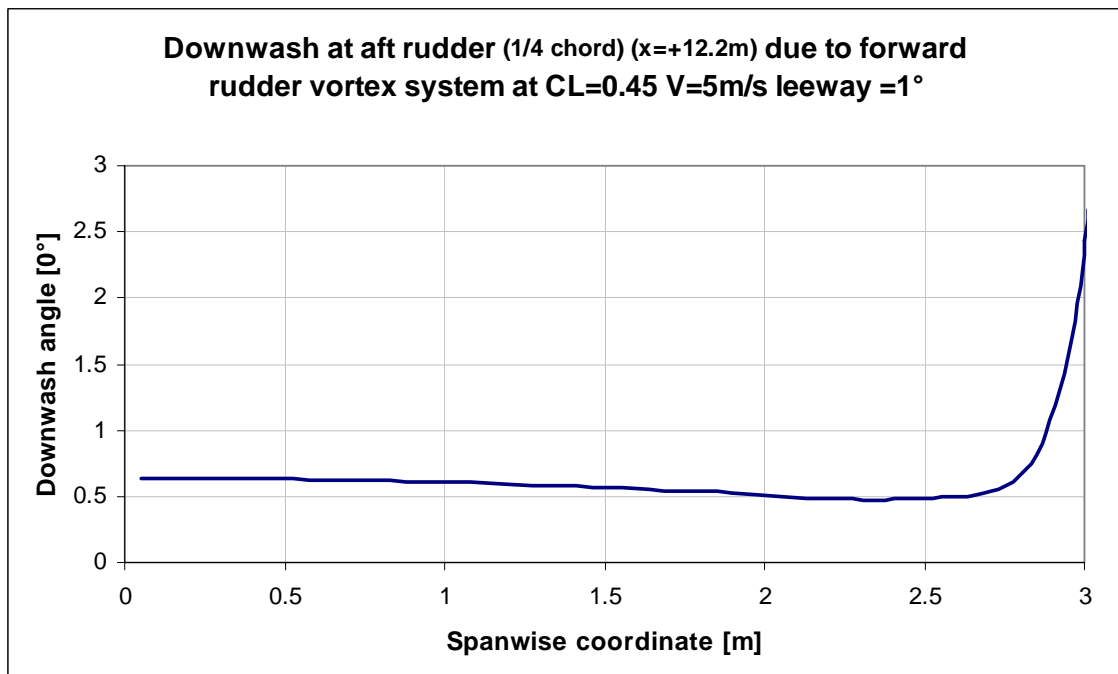
Diagram 07.b

As expected eq. 07.4 is influenced by the position of  $y_1$  in the X axis, it will be influenced both by  $\alpha_1$  and  $\alpha_2$ , the following graph (07.3.b) shows the influence of the bound vortex on the downwash angle for a typical strength, the effect quickly to small values.



Graph. 07.3.b

The second program used the circulation distribution from the lifting line and computed the influence of all the vortices on a specified point. This gave Graph 07.3.c which represents the downwash at the x position of the aft rudder ( $x=12.2\text{m}$ )



Graph. 07.3.c

The above graph shows that the aft rudder will not be in a uniform flow, therefore the elliptical planform will not give minimum induced drag. The above downwash distribution at the aft rudder requires that the planform produces more

upwash (from its own bound circulation) at the root and at the tip; this requires a less tapered planform.

The above downwash distribution can be fed back into the lifting line program as an angle of attack distribution, or to make it easier as a twist distribution of the wing.

The aft rudder was then designed to get an elliptical lift distribution (constant downwash) for minimum induced drag, which in the geometry is traduced by an increase in tip chord to increase its own upwash. Another way to increase tip loading would have been to increase sweep angle of the wing, this could mean that the same geometry could be used for the aft and forward rudder therefore a decrease in costs. However lifting line theory is not able to handle sweep angle. Such investigation would require a vortex lattice program, some are available from the internet but they were not found friendly enough to use for such investigation. Such program is in development by the author, and will be used to investigate such design at a later date.

*The lifting line program lines is shown in the appendices A4.*

### **07.3.7.3.3 Other influence**

The hull will influence the flow field between the rudders, the first is viscous related, the aft rudder being at the back of the boat the upper part of the rudder might be in the wake of the hull, the wake will be thin at most leeway angle and its influence is seen as limited. The second influence of the hull is that the hull surface being curved will change the downwash shape, on such light displacement yacht buttock lines are straight and the last influence is seen as small. Finally, when the hull has a yaw angle to the flow a cross-flow of twice the yaw angle can be expected on its body (*see diagram 07.2a*), this effect will influence the vortex sheet shape and therefore the downwash. As the expected leeway angles are small, the last effect is again small and neglected.

Several aspects of the downwash is not modeled by the lifting line theory.

The trailing vortex sheet is assumed to originate at the lifting line and to extend unchanged to infinity. Several effects influences and make the last statement inaccurate, they are known as rolling up, distention and distortion. Their influence will be to change the shape of the vortex sheet. It was found in [13], that it was accurate enough to not take into account their influences for such large separation between the two rudders. An area of investigation is the amount of contraction of the tip vortex and its influence on the aft rudder, such influence has not been researched (or available) since most plane tail wing is very close to the main wing (maximum is one span).

Actually an advanced vortex lattice code, which model wing interaction, does not take into account such effect.

#### **07.3.7.3.4 Conclusion**

Such program gives great insight into planform design, the optimization of the rudders planform. Moreover the forward rudder tip vortex will roll up and the velocities will be different from what the theory gives. It is not known how the hull and waves influences the direction and path of this vortex, it is known that the hull affects the keel vortex by what is called contraction and therefore the keel span is reduced. A problem would appear if the forward tip vortex comes too close to the aft rudder. It would mean that a limited amount of leeway is beneficial.

### **07.3.8 Viscous interaction**

#### **07.3.8.1 Introduction**

Inviscid interaction (leading to induced drag) was treated above (07.3.6.3). Viscous interaction is believed to play an important part too. Viscous interaction will be most important at leeway of  $0^\circ$ , where the wake of the forward rudders meets the aft rudder, it reduces velocity and therefore drag will be lower. It is not known however how it will influence the performance when a leeway angle or/and a rudder angle is present. Viscous effects are best investigated with RANSE solvers.

#### **07.3.8.2 Investigation**

A RANSE investigation of the viscous interaction between the two rudders, was planned and begun, but it was soon found that the time needed to complete an accurate investigation was too important to be pursued in such project. The process involved building 2D structured mesh of 2 foils sections situated 12.2 m apart as in the final design. The first mesh contained 121000 elements. The difficulty of such mesh is to make sure that enough cells are presents to 'bring' the wake to the aft rudder.

As seen before the vortex sheet (which is situated at the same position as the wake) cannot be predicted well by potential flow, its position does not affect much the downwash angle calculation but the wake position is important. Such 2D investigation won't give accurate position of the wake. A 3D investigation was not possible due to the size of the mesh that will be required. Using the same mesh quality (still found not accurate enough to get good section drag coefficients) would have required at least 24

millions cells to span the two rudders, which is well above what today's computer can cope with.

However it was confirmed that the wake will actually go up to the aft rudder at the speed tested (5 m/s). Therefore at zero leeway and at another leeway angle the wake will interact with the aft rudder. This is due to the downwash distribution and viscous effect that when leeway is  $0^\circ$  and the rudders have an angle of attack, the wake will actually pass to leeward of the aft rudder. With increasing leeway angle the wake will come to windward of the forward rudder. More detailed investigation need to be done, to investigate the point where the aft rudder crosses the forward rudder wake.

### 07.3.9 Structural design

*(see spreadsheet in appendix p A6)*

Structural design is an important part of rudder design. Rudders are highly loaded structure members, and as such structural design is often considered as more influential on the rudder design than its hydrodynamic efficiency. The rudder needs to rotate through two bearings, therefore a rudder stock need to be used; high strength carbon will be used to reduce its size and weight to a maximum. Materials characteristics were taken from manufacturer literature [14] with a downgrading value of 1.3. The design was done taking ABS as basis for a more advanced spreadsheet, the worst case scenario taken into account to size the stock will be a broach at 21 knots ( $F_n=0.75$ ) of boat speed. The assumed rudder stall  $C_{LSTALL}$  is 1.2 for such high aspect ratio. The pressure distribution on the rudder was assumed to be proportional to the chord distribution which is correct for planform close to parabolic, this assumptions gives a better estimate of the centre of pressure and forces involved. Stock failure could be catastrophic if it breaks into the boat, it would mean complete flooding of one compartment, therefore some factor of safety of different value have been applied along the stock to make it break at 900mm under the bottom bearing, this should remove any chances for breakage of the stock in the boat, the values used are as specified by [15]. Then the rudder stock was modeled checking both bending moment and shear forces requirement. The rudder blade is able to carry the bending moment loads at 1.8m below the root, for load transition the shaft will go until 2.1m below the root.

### **07.3.10 Conclusion**

The rudder design shows well how structural design and hydrodynamic design are inter-related for such cases. This is actually an iterative process. The different theories and tools used here were of great interest by the author.

## 07.4 Canting Keel

*See plan VO70-A1*

### 07.4.1 Introduction

The keel could be thought to be the most adapted source of sideforce, due to its maximum span (high AR), its position in the middle of the boat (good for yaw equilibrium). Unfortunately there are many drawback to its use; at hull speed ( $F_N=0.38$ ) a wave hollow is present at the middle of the hull, the keel producing sideforce produces a negative pressure on its upper side hence for equilibrium bring the free surface closer (increases wave drag). Moreover the influence of the bulb on effective span is not good; a bulb does not act as an endplate, it actually reduces effective span by 5 to 10 % [17]. Finally the use of the keel as a canting strut to move the ballast sideways decrease the effective span by a bigger amount, this effect is similar to the dihedral angle of tail wings on airplane. Moreover when canted it will produce lift directed upwards and counteract righting moment. It is then obvious that the keel is not effective for producing lift.

### 07.4.2 The rule

The main influences of the rule on the design are:

2.16.4.b The ballast keel can be canted up to 40 degrees

2.16.4.g Bending and shear stresses shall be calculated for the keel sections due to the transverse bending moments and shear forces that arise with the keel and bulb horizontal and out of the water. The minimum factor of safety for the associated stresses shall be 3.

2.16.5.a Only steel, steel alloys and/or bronzes are permitted in the basic construction of the keel fin. For design purposes the tensile yield strength is not to be taken as greater than 390 MPa for steel.

### 07.4.3 Lateral area requirement

In the case of the daggerboard configuration, in light weather the keel is not canted therefore the keel can be used to produce lift, and the daggerboard can be lifted out of the water. Therefore to limit leeway the keel area needs to be of a minimum area.

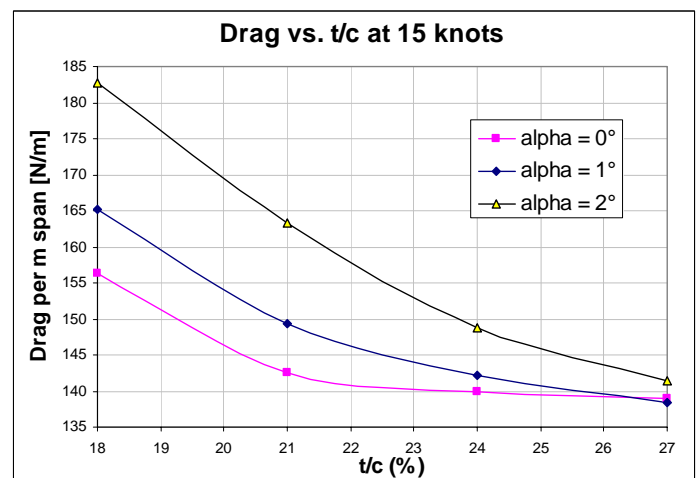
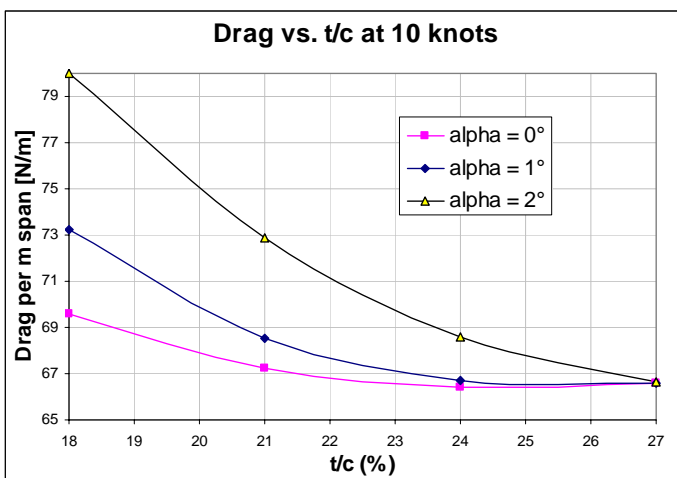
In the CBTF case the aft and forward rudder cannot be retracted and will produce the necessary side force. Therefore the keel will not be required to any sideforce and can be designed as a simple strut.

#### 07.4.4 Keel section thickness choice

The canting keel has no role in producing lift. Its role is to produce righting moment by holding the bulb. The two main axis of design for such appendage optimisation are drag and structural requirement.

As thickness increases, for the same I value, chord can be decreased; frictional drag goes down (less wetted area), but pressure drag increases (t/c ratio increases).

A study can be done using a spreadsheet, a Cad program (to get Inertia), and a section design program (to study the section characteristics with t/c and Re varying). The program used is called Xfoil, it is a 2D panel method with an  $e^N$  method to handle boundary layer development, and it is seen as the most evolved 2D section design software (although being free). This quick study yields the information given in graphs 7.4.a.



Graphs. 7.4.a : Drag vs. t/c keel section design

These graphs show that going for a high t/c is beneficial. Increase in pressure drag is lower than decrease of frictional drag. A possible problem with such high t/c is boundary layer separation; as the fluid goes around the section at the maximum thickness pressures decreases, then the pressure increases if this positive pressure gradients are too high, separation can occur. Unfortunately it was not known if the 2-D Panel Method program could predict separation very well, and most importantly its

influence on drag. Research had to be done to enquire about the separation behaviour of such foils. A NACA [16] report was found dealing with the wind tunnel testing of such thick sections. It confirmed the numerical above results, and confirms the good behaviour of Xfoil viscous estimations.

An advantage of such section is their very wide drag bucket. Profile drag does not change between  $\alpha = -3$  and  $3$ .

Moreover as  $t/c$  increases, keel weight reduces by up to 11%.

The section chosen will be a 641022, the section has a drag bucket that extends up to  $C_l$  of 0.11 and shows a very low base drag coefficient ( $C_{d0}=0.00613$ ), it should work well at the expected low angle of leeway. It also shows a flat pressure distribution which handles well cavitation.

### Cavitation

Cavitation occurs when pressure on the surface of the foil becomes so low that water vaporises and vapours filled cavities forms, it often seen on propeller blades. It will increase drag and cause erosion. It must be avoided. Cavitation on a thick section is most probable to occur than on thin sections since the pressure loss is higher ( $V/V_\infty$  is higher). A speed of 30 knots was chosen as the limit where cavitation was accepted to occur. Critical velocity is related to pressure by the following equation:  $V_{CRIT}=(195/(N_{cav}))^{0.5}$  where  $N_{cav}$  is the cavitation number and is equal to  $-C_p$  the minimum pressure coefficient of the section. Therefore if  $V_{CRIT}=15.44$  m/s (30 knots)  $C_{pMIN} = -0.81$ . The next step was to find the maximum  $t/c$  ratio which has a  $C_{pmin}$  of -0.81. With the aid of Xfoil, taking into account an angle of attack of  $1^\circ$ , the maximum  $t/c$  ratio before cavitation was 22%.

### 07.4.5 Structural requirement

For the best compromise between weight, wetted area and precision and rule requirements, a forged steel construction was chosen. The piece will be machined to the required shape.

The keel can be idealised as a cantilever beam with a point load at the end (the bulb) and a distributed load over its length (fin weight), as the fin is not constant in cross section the distributed load wont be constant. A spreadsheet was written to design such structure. The following table shows the structural characteristics of the keel at different depth.

Coordinate	BM [kN.m]	Zachieved/Zmin	t/c
0	261.80	1.06	0.22
500	222.13	1.00	0.22
1000	183.77	1.03	0.22
1500	146.68	1.03	0.22
2000	110.76	1.04	0.22
2500	75.92	1.06	0.22
3000	42.06	1.19	0.21
3400	15.64	1.92	0.20

Deflection was checked as well, a program was written to take into account the decrease of second moment of area from root to chord, a deflection of 70 mm was found (90° heel), and corresponds to a Length- deflection ratio of around 50, which is believed to be reasonable.

*See spreadsheet details in appendices (page A8).*

#### 07.4.6 Keel fillet

Simply attaching the (straight) wing to the bulb or keel will cause a large separation region near the junction, where the hull boundary layer encounters the strong pressure rise of the keel stagnation region. The common measure to eliminate this separation is by applying a fairing of suitable shape at the junction. In the present context there is a second consideration in the design of the fairing, namely that of the contamination of the laminar keel by the turbulent boundary layer on the bulb or keel.

The other idea behind fillets are the decrease in t/c ratio, interference drag is present when a wing crosses a wall (keel-bulb and keel-hull), such drag is proportional to  $t/c^3$  therefore it is interesting to decrease t/c at the junctions of the bulb and keel and at the junction of the keel and hull.

As shown on Lurie [9], the keel/bulb junction can produce necklace vortex around the fin/bulb junction which trips the boundary layer to turbulent.

#### 07.4.7 Planform shape

The planform shape is mainly product of the structural requirements. Any twisting due to the bulb is not allowed by the rule. Therefore, the keel taper, sweep back and section t/c have been tweaked to produce a twisting neutral fiber (the centroid of the section) the straightest possible. Leading edge sweepback is constant and minimal to promote laminar flow on the forward part of the foil.

#### 07.4.8 Canting keel mechanism

As said before the canting keel mechanism will need to cant the keel through  $80^\circ$  ( $2 \times 40^\circ$ ). The rule requires two independent canting systems (two hydraulic rams here) with one manual override. Canting keel mechanism can be built from scratch or a complete system can be bought. In today's technology, the Volvo 70 canting keel mechanism won't be different from what is seen on current boats. Bulb weight and canting keel are similar (if not less) than current boats. However some weight saving will be required as the system is still heavy.

#### 07.4.9 Practical consideration

Another advantage of decreasing planform area is that lift is reduced. At high speed downwind, with varying pitch angle, the keel might have a negative angle of attack and then reduce righting moment. This is a possibility, but the author is not aware of such things happening in the Open 60 fleet. Due to the limited area less force will be provided for the same angle of attack. This will decrease the possibility of this problem happening.

#### 07.4.10 Conclusion

The keel on a Volvo 70 has a different role compared to "normal" yacht where its role is to produce the main part of the side force; as such the finished "optimum" design is different.

## 08 - Towing tank

### 08.1 Introduction

The idea was mainly to compare 2 different appendages configuration (see dia. 08.a) on the same hull. It also gave an insight in canting keel behaviour. Towing tank was jointly done with a fellow student (Antoine Gautier), it enabled to do more than 400 runs. (2 days each)

Extrapolation to full scale was done to compare real forces. Extrapolation technique follows general rules. The rudders had laminar flow in the towing tank hence have scaled this into account.

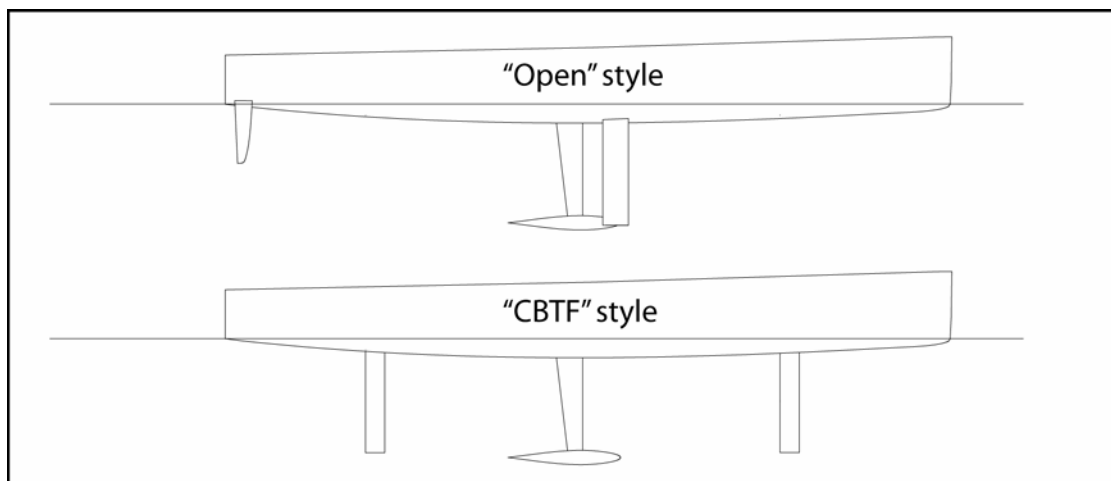


Diagram 08.a

### 08.2 Model used

The model scale chosen is dictated by many factors, mainly the tank size, the available budget and time scale. It is known that bigger model gives more accurate results. The model scale chosen was 1:10, which gave a model length of 2.15 m. Blockage is not an issue since the model cross section area is  $1.23e-2 \text{ m}^2$  well inferior than tank cross section area / 100 ( $6.66 \text{ cm}^2$ ). Maximum towing tank velocities should be lower than the 0.7 the critical wave velocity ( $(gh)^{0.5}$ ) which give a maximum full scale speed of 18 knots. (as advised by De Bord et al. [18])

### 08.3 Model design

Tank testing was scheduled early, so hull design was not finalized by that time. It was decided to adopt a “middle of the road” approach and choose a conservative hull at the overall beam of 5.2m which is the mean value of the permitted  $B_{OA}$  (4.7 to 5.7). The parameters of the hull are the following:

LOA	2.15	m
LWL	2.08	m
BWL	0.3822	m
Tc	0.049	m
Vol	0.01462	m <sup>3</sup>
Cp	0.57	-
LCB	5.65	%
WSA	0.5774	m <sup>2</sup>
LCF	6.02	%
T	0.46	m
WA	0.512	m <sup>2</sup>

### 08.4 Appendages tested

As explained above two main configurations were tested:

An “open style” configuration which consist of twin rudders aft to generate the turning moment to steer the boat, a canting keel to generate the righting moment, and an asymmetric daggerboard generating most of the sideforce. This is seen as a better approach than the similar one where there is a single symmetric daggerboard on the centreline (see appendages chapter). The configuration used is the common approach for open 60 and Mini-transat; it has shown reliable results around the world and for short handed racing.

The second configuration which is known as Canting Ballast Twin Foil (CBTF), it consist of a canting keel generating righting arm and two rudders situated fore and aft the keel on centreline generating the required lift and steering the boat.

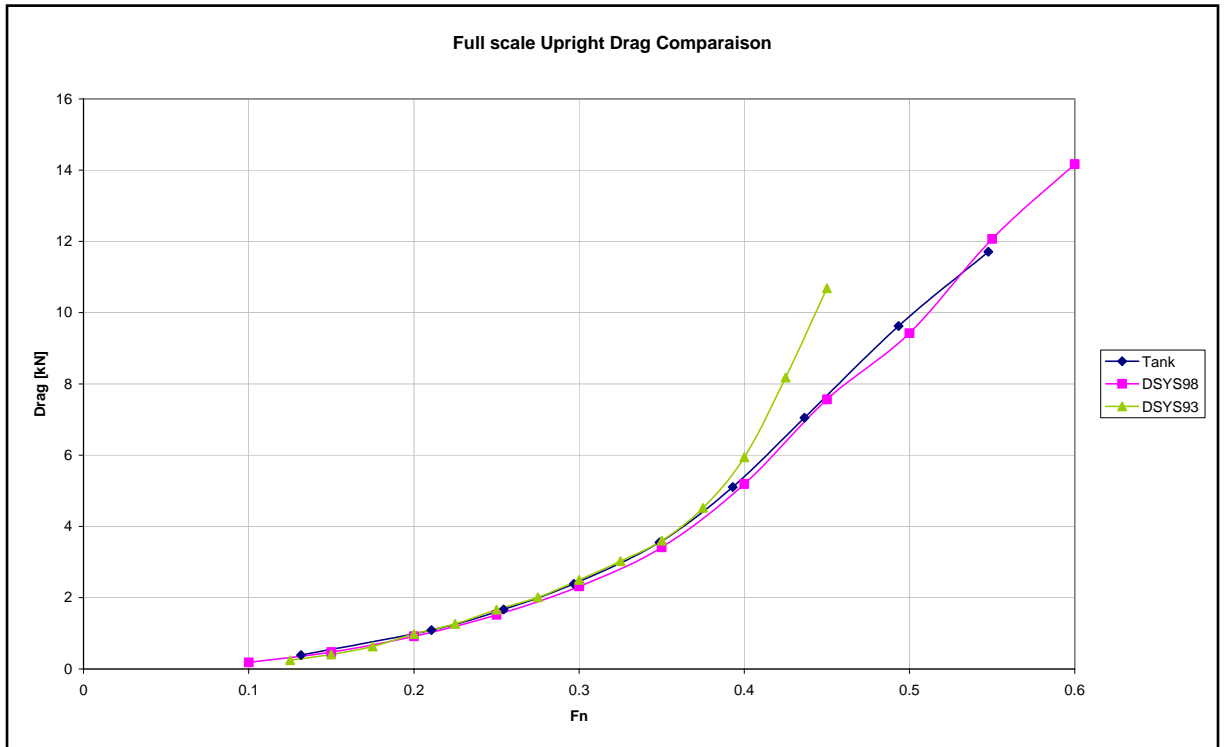
Theoretical and practical advantages/disadvantages of the two configurations are explained in the appendages design chapter.

To limit the influence of viscous terms, all the appendage were designed using rectangular planform and 00series Naca section.

## 08.5 Extrapolation

Extrapolation to full-scale was required to be able to regress the data and put it in the Vpp, it gives as well a better way to compare the boat. Extrapolation was done following common practice. The total model resistance is measured, the viscous resistance of the model is calculated using a 2-D friction line method (here ITTC 57 using a characteristic length of  $0.9 \cdot L_{wl}$ ) and a form factor (found using Prohaska method) representing pressure drag. The balance between measured drag and viscous drag is determined to be residuary resistance. The residuary resistance is extrapolated to full scale using Froude scaling ( $scale^3 \cdot \rho_{fullsize} / \rho_{model}$ ), while the viscous resistance is scale using the same friction line method but with a different the full size  $R_N$ .

It is always interesting to compare upright resistance to the one predicted using the Delft series. As shown on graph 08.a, agreement is very good, particularly for the last one. It is interesting to note that the model tested is at the limit of the Delft database (due to the high length displacement ratio and  $L_{wl}/B_{wl}$ ). Curves start to diverge at the highest speed, probably due to the high length/displacement ratio of the boat. Delft series are the basis algorithm to compute wave resistance of hulls in a VPP, it is confident to see that they are reliable for this kind of hull. At the lower speed, where frictional resistance is the main part, the agreement of results shows that the ITTC 57 formula for estimating friction drag is accurate.



Graph 08.a

### 08.6 Canting keel influence on upright resistance

When the keel is canted to the maximum 40°, an increase of residuary resistance is expected and was seen in the tank. The volume of the keel and the bulb being closer to surface interact and increase the wave around the boat. The following table (08.a) presents the total full size drag increase due to the keel being canted to 40°. In sailing terms it corresponds to 30 more hours on a round the world race.

Fn	Drag increase due to CK at 40°
0.254	3%
0.297	3%
0.349	3%
0.393	4%
0.436	4%
0.493	2%
0.548	2%

Table 08.a

A graph of the upright resistance for the two cases is presented in the appendices. (Graph 19.a page A9)

At the higher speed, the situation is reversing for the model tested. It can be explained by the fact that the canting keel when fully canted is producing upward lift, therefore reduce apparent displacement (hence wave drag) and wetted area. However this answer would not be correct in sailing condition because upward lift on the keel will increase heeling moment. It is not possible to measure heeling moment in the tank, and not enough run were done at high speed to investigate the trim and heave value with confidence, but this an area which needs more study. As seen on the next table the situation reverses at around  $F_N=0.665$  or 19 knots.

<b>F<sub>N</sub></b>	<b>Drag increase due to CK at 40°</b>
0.548	2%
0.665	0%
0.776	-2%
0.884	-4%

## 08.7 Influence of forward rudders on wave resistance

As said before in the rudders chapter, the aft and forward rudder (the forward to a greater extent) have an influence on wave resistance, at a  $F_N$  of around 0.4 they should reduce wave resistance.

In the tank the influence of the rudders on the waves was visually seen, and the influence of the forward rudder is important. However, in quantitative term, the process to see its influence is more difficult. It is not possible to compare directly with rudder and without because induced drag and viscous drag will be different. Therefore, induced drag need to be calculated and compared, as is heel and viscous drag. These steps bring inaccuracies and the small amount of expected decrease in resistance is masked by these errors.

## 08.8 Conclusion

Using the towing tank was of great interest in the project, this is a time consuming tool but worthwhile in such project. It has been very rewarding to know the limitation of the tool and the degree of accuracy in its use to yield good results.

## 09 - VPP investigation

To fully compare the two configurations, it is needed to analyse using a VPP. As seen before the CBTF approach has an edge upwind but lack the capacity of removing the daggerboard downwind. Experimental results are determined at discrete conditions (heel, yaw and speed), whilst the Vpp requires a continuous definition of behaviour. The data needs to be regressed using the method shown below.

### 09.1 Resistance breakdown in WinVPP

$$R_{tot} = R_U + R_U(c_1 + c_2 V_S + c_3 V_S^2) \varphi^{c_4} + F_H^2 / V_S^2 (c_5 + c_6 V_S + c_7 V_S^2 + c_8 \varphi^2)$$

$$R_{tot} = R_U + R_H + R_I$$

$c_1 - c_8$  = coefficients determined by regression analysis

$R_U$  = Upright resistance

$R_H$  = Heel drag

$R_I$  = Induced drag

$V_S$  = boat speed

$F_H$  = heel force

$\varphi$  = heel angle

It is obvious that representing the boat hydrodynamic behaviour with such low number of coefficient is difficult and will yield errors. However, increasing the amount of coefficient used could improve the accuracy of the regression method but it creates 2 main problems; first, as the numbers of terms increases it becomes harder to ascribe a physical significance to each one, and, secondly, it becomes impossible to extrapolate the coefficient reliably beyond the tested matrix. Such method is time consuming, discrete combination of heel angle and speed need to be chosen to best fit the data. (Low speed with low heel angle). Then the expression needs to be checked to ensure consistent behaviour of predicted resistance outside of the range of the test points. It becomes more difficult when the data is needed to compare two different boats as are

the Cbtf and “open” style, the difference in appendages configuration will change how the boat is sailed.

Considering the whole evaluation process of the two hull forms the regression is the most inaccurate link.

The author wishes to thanks G. Barkley for providing a spreadsheet that made the process easier.

## 09.2 Comparison of the two configurations

Some of the towing tank results were found not accurate enough particularly the results of resistance related to the cbtf were it was found very difficult to be exact about the alignment of 3 appendages of less than 5 cm of chord. Therefore for the comparison the open configuration was taken as the basis and frictional drag was added for the rudders.

In the tank the daggerboard used for the open style was one from a past open 60 project and was too small to generate the optimum sideforce. Similarly the cbtf rudders were found to generate enough sideforce, so it was possible to reduce they area. The scaling in terms of effective draft is not straightforward since it affects the whole configuration.

### **09.2.1 Change of daggerboard area and rudders area**

A vortex lattice method program called Tornado [19] was used to get the required factors. Such program is able to model a complete system of wings, with their potential flow interference (no viscous interference). The process was found important since it takes account of the whole appendages configuration. The hull was modelled as a low aspect ratio wing and all other appendages as in the tank. Increase or decreases in viscous drag were more straightforward, and were done considering only the change in surface area and Reynolds number of the section.

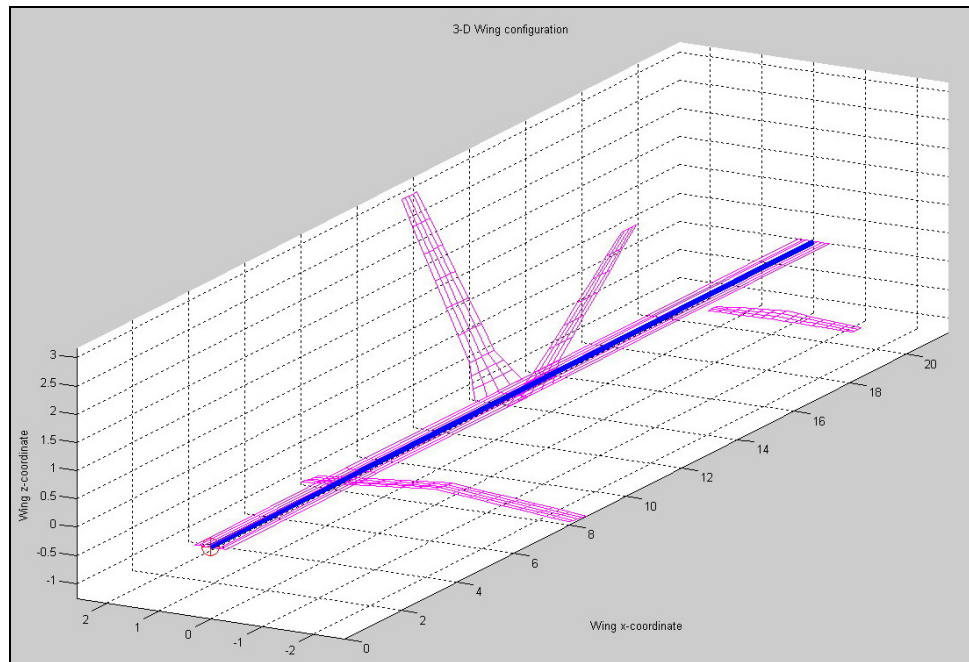


Diagram 09.a - Configuration “Open” Canting angle 40°

The free surface was assumed rigid ( $F_N=0$ ). One of the main requirements is obviously to have zero velocity normal to the free surface, this was satisfied by mirror imaging all of the elements about the plan of the free surface (*see diagram 09.a*).

Calculations were done at 3 different yaw angles for all configurations to yield effective draft of each one.

These results were used to change the effective draft due to the increase in depth and area of the daggerboard, or the decrease in area and depth of the CBTF rudders. The results were used to change the tank results. With the many assumptions, the method above used alone without tank testing would probably bring significant errors.

Using the method above to extrapolate the results, the main assumption is that the change of geometry does not affect or is affected by the waves, which is true since most of the geometry changes is in span, therefore deep under water.

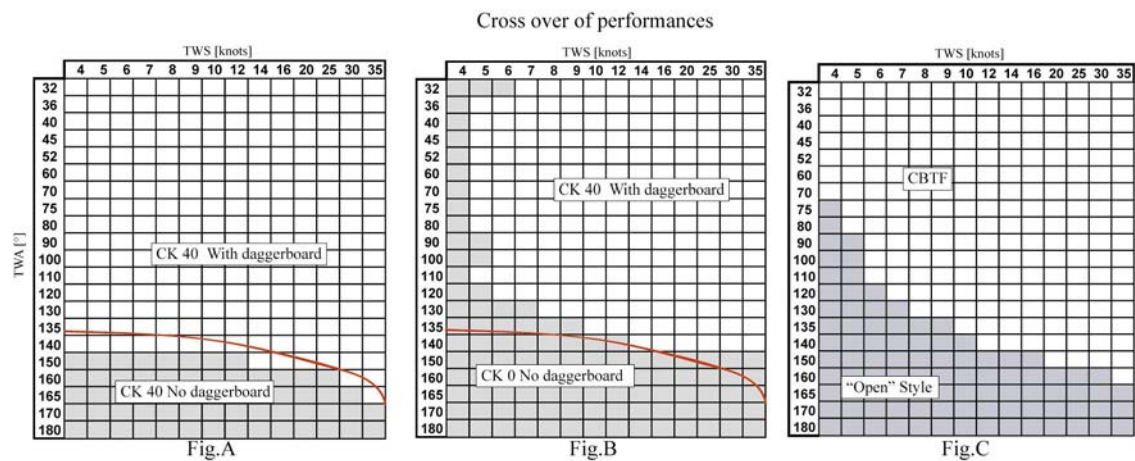
### 09.2.2 Results

At the end of this process, it was found that the cbtf had a lower wetted area when the daggerboard is down. And still has a better effective draft, therefore performance is better. However the daggerboard can be lifted out of the water, and in lighter wind or downwind wetted area can be reduced.

An intermediate level of canting keel angle was tried to see if increase effective draft could be exchanged with less stability but it was not successful in term of performance.

The configurations tested in the VPP were:

- CBTF with reduced area of appendages
- Twin daggerboards with increase in span to increase effective draft and area
- The keel canted at  $40^\circ$  without daggerboard (expected to represent downwind)
- The keel canted at  $0^\circ$  without daggerboard (light upwind and dead downwind)



The above figures represent the different cross over of best speed. Fig. A shows the true wind angle (TWA) when it is beneficial to remove the daggerboard. As expected the cross over is only for high angles. The cross over is actually below the VMG angle downwind.(Red lines). It shows that for such high powered yachts, with large asymmetric spinnakers. Removing the daggerboard downwind is not beneficial in terms of VMG. The advantage of lower resistance doesn't make up for the large loss of lifting area.

Fig. B shows the cross over in performance between the keel canted at  $40^\circ$  and the daggerboard down, and keel canted at  $0^\circ$  but no daggerboard fitted. This is a trade of between, viscous drag, stability and effective draft. As expected in light winds when no large righting moment is required, the advantage of lower viscous area is beneficial in terms of speed. However such advantage is quickly lost since the boats are quickly powered and stability is required.

Fig. C shows the cross over line (red line) between A CBTF and an “Open 60 style” configuration. The open 60 style is the configuration where the daggerboard are set up to give the best performance (lifted in light wind,etc...). As expected the “open style” is good off the wind when the daggerboard can be lifted to reduce wetted area, but in most areas the daggerboard system lacks the efficiency of the cbtf in producing side force.

A polar plot for both configurations is shown in the appendices (*polar plot page A9*), it clearly shows that the advantage of the daggerboard is at angles larger than the best VMG downwind for wind speed above 10 knots.

Some other configuration with the daggerboard being lifted at different increments (75% 50%) where tried but didn’t give significant increase in performance.

Finishing time advantage of CBTF over Daggerboard	
Legs	% diff.
1	1.1%
1a	2.7%
Inshore	2.1%
2	-0.4%
2a	-0.3%
2b	-0.5%
Inshore	2.1%
3	2.1%
4	0.4%
4a	0.7%
Inshore	2.3%
5	1.4%
5a	0.8%
Inshore	2.1%
6	0.0%
7	-0.6%
7a	-0.6%
Inshore	1.9%
8	0.4%
Inshore	2.1%
9	-3.6%

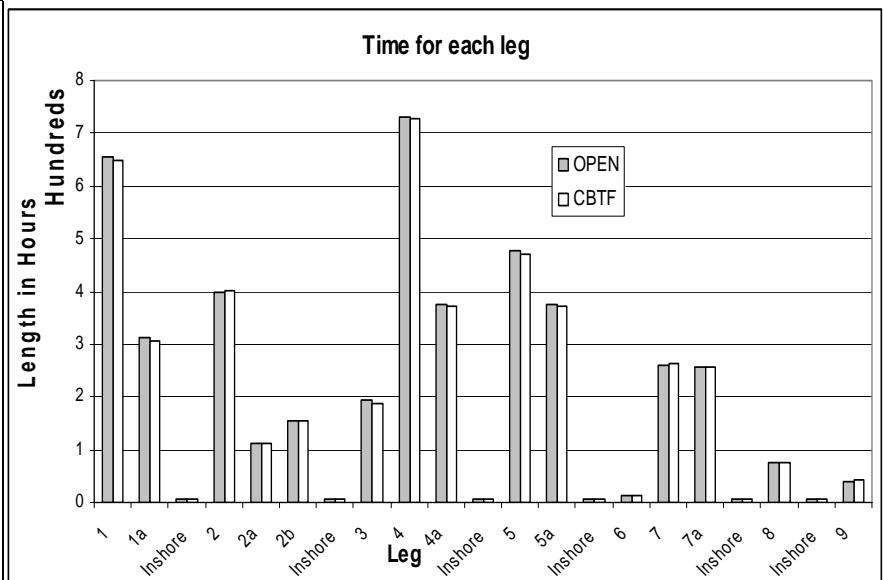


Table 09.a and Graph 09.a

The above graph (9.a) shows the finishing time expected for the two configurations in function of the leg. The table represents the time difference (in percentage) advantage of the CBTF over the daggerboard configuration. As expected the CBTF is always the best in the inshore races. But do quite well on many offshore too. In the case where the races are mostly downwind (leg 2) or/and in light winds (leg 7 and 9), the daggerboard configuration takes the lead. However using the coefficient

for the legs (0.5 for inshore and offshore gates and 1 for offshore finish), the CBTF configuration is by far the best. (10.5 vs 5 points at the end of the race). As seen above the time differences are very low (mean value of 1.5% of leg length), around the world the difference sums up to a difference of 15 hours if only the offshore races are taken into account.

### 09.3 Discussion

It was found that the fact that the keel has to be built out of steel has quite a big effect on the choice of appendages, as seen above the frictional resistance of the two rudders has an important effect in the lighter winds on the performance. Reducing the keel wetted area with a move to high tech composite will see the cbtf configuration in a better position.

### 09.4 Choice of appendages

Choice of appendages is down to very small things. The main problem with cbtf is in case of collision with a submerged object. The loss of the forward rudder is evident. Twin daggerboards system will always have the advantage of the possibility to swap the broken one. Carrying a smaller forward rudder is a possible option.

Turning ability with the CBTF will be increase, the common trend in open boats is to move the keel aft therefore the turning lever (d between rudder and keel is reduced). For the cbtf boat the turning lever is between the two rudders. This will significantly increase the ability to steer at low speed, and will be a significant advantage for the start of the inshore races.

Performance in waves of the system are difficult to gauge, but from experience with Wild Oats (a CBTF 60'), its designer says that cbtf is very well behaved and performance gain are similar in waves as in calm water. [20]

## 10 - Rig design

*See plan VO70-SPDP1*

### 10.1 The rule

**6.1.1 (a)** External mast dimensions (below IG) shall not be less than 300mm fore and aft by 150mm, or greater than 375mm fore and aft by 180mm wide.

**6.1.2** Mast weight not less than 625 kg and centre of gravity not less than 12.000 m above mast datum.

**6.2.8** Chain Plate width (for V1s) shall not be less than 4.000 m.

### 10.2 Choice

Deck beam at mast position is 4.106m, so it is close to the minimum of 4.0m. The spreaders will have a 9° of sweep back. This is a compromise between longitudinal support and mast tweaking simplicity. It was thought that a minimum of longitudinal was needed to decrease the probability of losing the mast with the low crew number.

The optimum number of spreaders was found to be four. As seen above the requirement in weight and section dimension are strict.

Rig measurement value (I, J, E...) have maximum value, to maximise sail area the maximum values have been taken. *See Figure 19.a in appendices page A10.*

### 10.3 Structure

Total weight is declared in the rule, therefore a complete study of mast structural design was not found worthwhile for a project where hull and appendages design were thought more important. However a check was done to see if the minimum was attainable with the minimum shroud base, as expected it was. It is interesting to note the minimum mast weight was changed from 675kg to 625kg. The former weight would have given credit to the use of rod rigging for the forestay over synthetic fibers as it stretches less. The weight of 625kg is attainable with complete Pbo standing rigging.

## 10.4 Weight Influence

Approximately for every 10 cm in increase of GM, an increase of 10 kg is seen in the rig. Obviously get the optimal weight, each rig configuration has its optimal righting moment.

Compared to the Volvo 60, the Open 70 sees the possibility of use of fibres to replace rod rigging. This corresponds to a gain of 12% of the total mast weight. This corresponds to 30 hours around the world. (1.2% gain). It shows the influence of reducing weight high situated and the advantages of switching from rod to pbo.

## 11 - Sail design

*See plan VO70-SPDP1*

### 11.1 The rule

The main aspects are:

- **7.3.9 Mainsail area**

$$MSA=29.75+7*MLW+7*MHW+5.25*MTW+4.532*MUW+2.783*MCW$$

*(See fig 19.b in appendices page A11)*

- **Part2, 2.9 (b) Amend. 03**

A maximum of 1 mainsail, 4 headsails, 2 storm trysails, 2 storm jibs, 2 reaching headsails and 4 spinnakers may be on board while racing. The maximum number of mast head spinnakers on board while racing shall be 2.

This last amendment removes the gennaker from the list of sails allowed, and therefore removes the Code Zero type sail.

### 11.2 Choice

11 sails are permitted for each leg (+ 4 storm trysails or jibs). The sail inventory has been chosen looking at similar boats (Volvo 60, open 60 and maxis). Areas are limited by the rule, so the sails are designed to the maximum allowed. Considerable amount of work need to be done to select the sails for each leg. A small amount of sails are available each leg, therefore they must perform well in several conditions. Wind tunnel testing has been extensively use in past Volvo ocean race campaign and will be used at a greater scale this time because 2 boat testing is not allowed. Sail design is seen by many as one of the most important part of the design for the next Volvo Ocean race.

Ideally sail design program would have involved sail makers, aerodynamicist and sailors. Sail performance characteristics usually come from CFD for upwind sails, whereas for downwind sails wind tunnel tests are the preferred method due to the high computational cost of downwind CFD simulations.

Obviously for this project, such facilities are not available. Such lack of information on the sails performance will affect the VPP calculation in quantitative term. The author does not think that it would change the hull and appendages design much. The main area of incertitude was the Code 0 sails, but such sails were removed in the 3<sup>rd</sup> amendment.

### 11.3 Design

The expected sail inventory is presented in table 11.a.

Mainsail shape has been designed to provide a fair amount of twist at the head. This will hopefully reduce the separated flow due to a large angle of attack. This will also reduce the top loading, hence reduce induced drag.

1	Mainsail	
4	Upwind headsails	
1	Asy Mashead Spinnaker	
1	Sym Mashead Spinnaker	
1	Asy Fractionnal Spinnaker	
1	Sym Fractionnal Spinnaker	
1	Medium Reacher	Code 3A
1	Heavy Reacher	Code 4A

## 12 – Hull Structural design

*Plan VO70-SBF1, LSI, SGA1.*

### 12.1 Rule

2.11 Minimum panel weight, excluding paint and fairing are specified for the hull, deck and watertight bulkhead

2.12.1 The maximum longitudinal dimension of any panel without internal support shall be 2.250 m.

2.15.1 The boat shall be divided into at least 6 watertight sub-divisions, in the location as specified in 2.15.1 (a) (b) (c) (d) and (e).

### 12.2 Design

The structural design of hull, deck has been done following the ABS Guide for building and classing Offshore Racing Yachts [21]. Other parts have been done using first principles. Contrary to hull design for example, optimisation is structural design is not possible, the loads are not well known, the materials used (carbon + honeycomb) are highly isotropic so most structural equation don't hold very well. The common solution is to let this work to structural companies like SP technology or High modulus, they are engineering most of the high performance boat and have a record what is working and what is not. This is for now the only way of optimisation; trial and error.

Panel weight and maximum stiffener spacing are limited by the rule. Therefore for the least weight, the way to go is to maximise the spacing. With this spacing it is still possible to pass the ABS panel requirement with the panel weight.

Hull and deck structural design was designed following strictly the ABS rule. Looking at the current state of the art racing-boats, it is clear that ABS rules are not entirely followed. (i.e. Monocoque structure) The author believes that experience is an important factor here. Any detailed structural design has not been done due to time constraints and difficulty of the subject. However basic calculations were done to estimate weights for the build up of the weight estimate.

The interaction between the tensile shroud loading and the compressive mast loads will be dealt with by structural solutions such as a V-Strap mast bulkhead, which effectively ties together the two opposing forces.

Core-Cell foam was chosen for the bow slamming region, for its great fracture toughness and fatigue strength. [22]

A sample of the results for the internals is shown in the appendices (*Page A12*). Panel calculation has not been included since using the minimum required panel weight; they are over build compared to ABS requirements.

Structural arrangement is shown in plan *VO70-SBF1* and *SGA1*.

### 12.2.1 Primary load influence

The main source of primary load is the loading from the rig. These loads come from the shroud tension to windward, the tension in the forestay and running backstays, and the compression loads at the mast step. The hull deflection due to these loads needs to be minimised to maintain forestay tension. There is also strength requirement; the increase in compressive stress in the deck (tensile stress in the bottom of the hull).

#### 12.2.1.1 Load estimation

The other source of primary load is the bending moment condition of sagging; when the wave through is amidships with the crest at bow and stern. Such load adds compression in the deck and tension in the bottom. Such configuration can be calculated with a stability software such as Hydromax, a sinusoidal wave 2.1m high (Height =  $L_{WL}/10$ ) was chosen. Then the program achieves equilibrium between weight, LCG, LCB and buoyancy.

Rig loads were found using the mast design spreadsheet; the maximum mast compression was taken as 50t. The rig loads are by far the biggest loads.

Shear force and bending moment diagrams are shown in the appendices (*graph 19.b 19.c page A14*).

#### 12.2.1.2 EI calculations

A program was written to calculate the EI value for all the sections. The hull geometry was input from an offset file. The hull was then divided into the different laminate areas. This made the process very fast, and changes on the laminate properties could be quickly assessed. The cockpit and coachroof weren't taken into account in the calculation, as well as the longitudinal stiffeners.

#### 12.2.1.3 Deflection

Deflection of the complete vessel could be calculated under load. Russell Bowler [23] states that "Providing hull panels are relatively stiff between frames,(and

hence section distortion limited), and there is sufficient material through topsides to offer good cross sectional area for shear, we have found simple primary bending calculations give results very close to actual bending tests on boats". This confirms that the calculated deflection should be close to the real ones.

#### 12.2.1.4 Results

This study showed that using the basic laminate from the rule would give too high stresses in the deck, and an important deflection (80mm at the bow and stern). It was therefore required to increase EI of the hull; the common way is to put carbon UD tapes the further away from the neutral axis, therefore at the deck and at the bottom. As the deck is further away from the neutral axis, more material is needed in the deck. The final choice was to add 2700g/m<sup>2</sup> of UD tape of 400mm width in the deck, it would decrease the laminate strain to approximately 0.14% (carbon failure strain = 0.5%) and would decrease fore and aft hull deflection to half the original value (44mm), such hull deflection increases forestay sag by approximately 500mm, this value was found a reasonable maximum for good upwind performance. This would increase hull structural weight by 80 kg. Wrinkling of sandwich face was also checked.

The panels laminate have been tailored to the requirement, the topsides panels have a greater amount of biaxial lay-up (+-45°) than on the bottom and deck panels. These +-45° fibres will increase the torsionnal stiffness and take the shear loads. 0 degree fibres are best used in the bottom and deck panel where it is further away from the neutral axis. (*See laminate schedule on plan VO70-LS1*).

*Graph 19.d and 19.e* in the appendices (page A15) shows the calculated EI value for the hull and deflection under the global loads.

*The method used above to calculate the loads and deflection is presented in [24].*

*Most materials properties are from [25].*

## 13 - Deck Plan

### *Plan VO70-SPDP1*

The deck plan was designed following the trend from past Volvo 60 project, taking into account the crew limit of 9 for offshore races and 10 for inshore. Additionally, up to three non-participating representatives from the syndicate, sponsors, or media may join the in-port racing.

The deck plan needs to be validated with the sailors. Deck plan is important in such advanced preliminary project for weight calculation.

Volvo open 70 deck plan design would be an important part for the crew, since the speeds expected are much higher, the loads are higher and the crew number lower than Volvo 60.

Following short handed boat cockpit design, the cockpit has been made deeper to provide more protection for the crew.

## 14 - General Arrangement

### *Plan VO70-GA1*

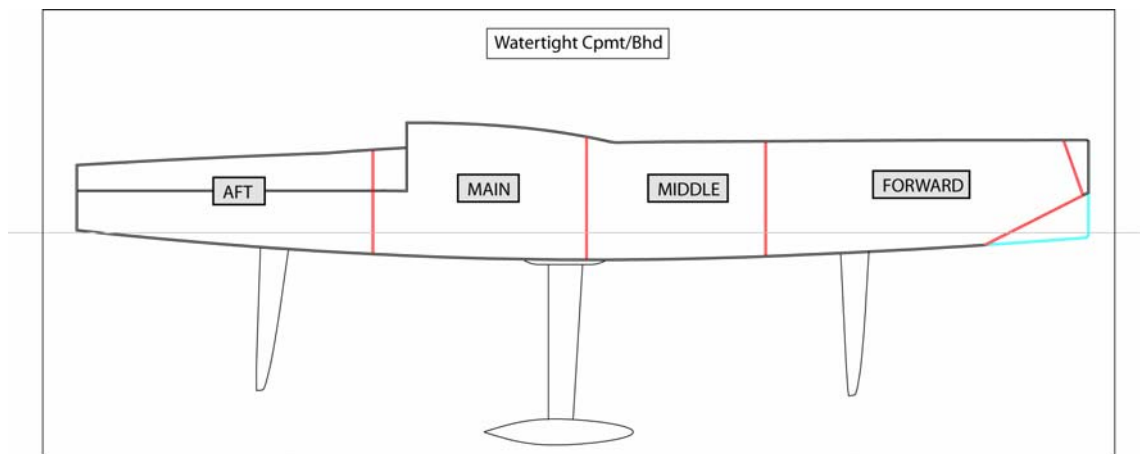
The rule is strict in the interior comfort requirements. It will improve the crew life in the boat, compared to past Volvo campaign where crews were known to lose considerable body weight through the legs. Space is still a premium in view of the canting keel mechanism and communication requirements.

## 15 - Stability check

*Rule Chapter 5 page 22*

There are two main requirements concerning stability in the rule. The first one is to have a minimum freeboard of 0.5 m with one compartment flooded. The second is a vanishing stability angle of  $115^\circ$  with the canting keel in the worst position. Stability characteristics were assessed using Hydromax from the Maxsurf range.

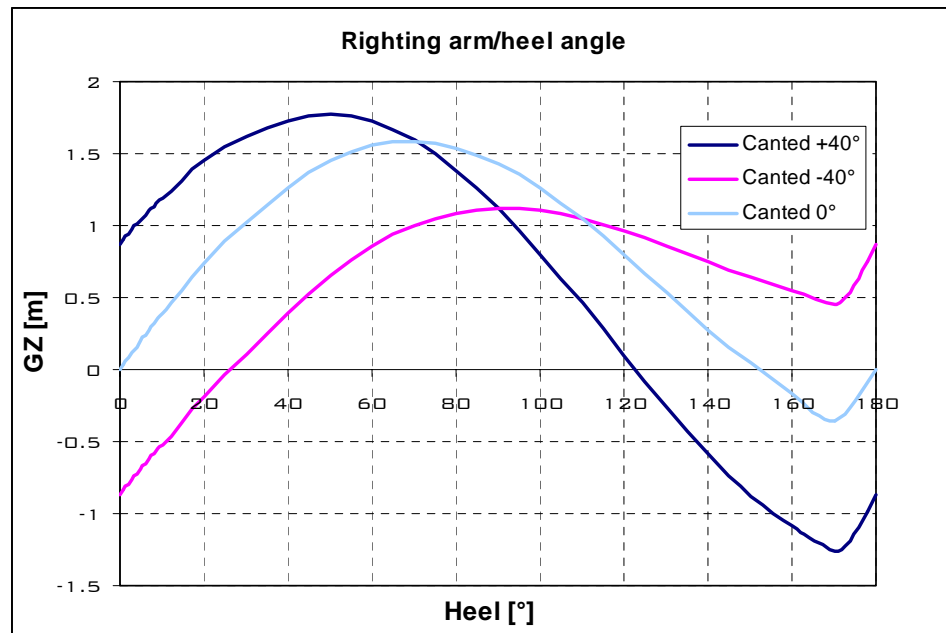
### 15.1 Damaged stability



Compartment	Flooded	Min Freeboard
Aft	0.633	m
Main	1.310	m
Middle	1.451	m
Forward	1.402	m

Damage stability is assessed using a light displacement + 2.5t added. The table above shows the minimum freeboard with one compartment flooded, the worst case is when the aft compartment is flooded but the freeboard is still at 0.633m (0.13m above limit). This is due to the compartment being quite big because of the forward position of the aft rudder. The rule requires a watertight bulkhead forward of the rudder stock.

## 15.2 Angle of vanishing stability



Large angle stability is assessed using the light displacement (afloat  $W$  in the rule). The graph above shows that the minimum vanishing angle is  $122.75^\circ$  with the canted keel in the worst position.

## 16 - Conclusion

Many things have been learned from this year long project. The main aspects of the project reflect the desire of the author to increase its knowledge in the field of aero/hydrodynamics and its tools. An important aspect of the project was Time management, time wasn't actually limited but many ideas were thought and not all pursued.

Many hours time have been gain by the fact that all software were used and mastered during the first and second year.

Each time possible an idea of the race time increase was given to have a quantitative idea of the change considered.

One of the main thing that was learn in this project, was to deal with time management. Many things can be accomplished in such project. But time is limited and a certain amount of time/worth needs to be chosen.

The total amount of hours spent on the project is estimated at 450 hours, with many more reading and researching.

### Suggestions for future work

A more detailed structural design will probably change the weigh estimate and influence the final choice of boat configuration.

Hull design and appendages design will benefit from more towing tank sessions, particularly in the influence of the canting keel at high speeds.

The author believes that work need to be done on VPP modelling of these new generation of appendages configuration. The author own VPP wasn't not finished in time to investigate in more detail the problem but this will be for sure an interesting work in the future.

Finally bulb design is still an unknown area of yacht design, but future advanced in RANSE turbulence modelling will probably change that.

The author has chosen to pursue its education into more advanced aero/hydrodynamics studies to investigate all these details in more detail.

Obviously the best way to assess the value of the present work will be to be at the start of the next Volvo ocean race and see how the boats look.

## 17 – References

1. **Volvo Event Management Uk Ltd**, The Volvo Open 70 Rule 2003, (2003)
2. [www.volvoceanrace.com](http://www.volvoceanrace.com)
3. <http://www.globalmarinenet.net/grib.htm>
4. WindPlot7.09 [www.xaxero.com](http://www.xaxero.com)
5. **Gerritsma, Prof. ir J., Keuning, Ir. J. A., and Versluis, A.** “Sailing Yacht Performance in Calm Water and in Waves”. 11<sup>th</sup> CSYS, (1993)
6. **J.A. Keuning, U.B. Sonnenberg** , “Approximation of the Calm Water Resistance on a Sailing Yacht Based on the 'Delft Systematic Yacht Hull Series’”. 14<sup>th</sup> CSYS, (1999)
7. **Hoerner, S H and V Borst** ‘Dynamic Lift’ (1975)
8. **Hoerner, S H and V Borst** ‘Drag’ (1975)
9. **E.A. Lurie**, “On-the-water Measurement of Laminar to Turbulent Boundary Layer Transition on Sailboat Appendages”, CSYS 15<sup>th</sup>
10. **H. Carmichael**,”Underwater drag reduction through optimum shape”
11. **Munk, Max M.**, "The Minimum Induced Drag Of Aerofoils", NACA Report No. 121, (1923).
12. **J J. Bertin and M L. Smith**, ‘Aerodynamics for engineers’ Prentice-Hall (1998)
13. **Silverstein, Abe Katzoff, S Bullivant, W Kenneth**, ‘Downwash and wake behind plain and flapped airfoils’, NACA Report 651, (1939)
14. Prepreg Technology, Hexcel composites
15. **Lochran**, “Structural design talk”, Southampton institute, (March 2004)
16. **EBullivant, W Kenneth**, “Tests of the NACA 0025 and 0035 airfoils in the full-scale wind tunnel “, NACA Report 708, (1941)
17. **N. Tinoco** “IACC appendages study” 11<sup>th</sup> CSYS, (1993)
18. **Debord, F. W. and Teeters J.** , “Accuracy, test planning and quality Control of sailing Yacht Performance”, New England Sailing Yacht Symposium, (1990)
19. **Tomas Melin**,” TORNADO 1.26b”, KTH, Department of Aeronautical and Vehicle Engineering
20. **Pugh**, Sailing World, “Article on canting keel”
21. **ABS**, “Guide for Building and classing Offshore Racing Yachts with notice n°2”, (1997)
22. **Tom Cowan**, 'The revolution is here' Seahorse (may 2004)
23. **Russell Bowler**, ”Construction Design Approach for Contemporary Yacht Hulls”, 6th CSYS, (1983)
24. **S. Wallis and R. Loscombe**, “Structural Design Learning Pack”, (2004)
25. **SP systems** Refnet Cd Rom version 7.

## 18 Bibliography

1. **Marchaj, C A**, 'Aero-Hydrodynamics of sailing' Adlard Coles Ltd, (1979)
2. **L. Larsson & R. E. Eliasson**, "Principles of Yacht Design". Adlard Coles Nautical, (1994)
3. **C. A. Marchaj**, "Aero-Hydrodynamics of Sailing". Adlard Coles Nautical, (1979)
4. **J. Gerritsma**, 11th C. S. Y. S., "Sailing Yacht Performance in Calm Water and in Waves". (1993)
5. **Cloughton, Wellicome & Sheno**i, "Sailing Yacht Design: Theory". Longman, (1998)
6. **Cloughton, Wellicome & Sheno**i, "Sailing Yacht Design: Practice". Longman, (1998)
7. **S. Wallis & R Loscombe**, "Structural Analysis Learning Pack". Southampton, (2004)
8. **Wallis & Patterson**, " Aero/hydro Hand outs", Southampton (2004)
9. **R. Loscombe & G. Barkley**, "Materials & Production for Specialised Craft". Southampton, (1997)
10. **S. Wallis & R Loscombe**, "Structural Design Learning Pack". Southampton, (2004)
11. **Abbott & Doenhoff**, "Theory of Wing Sections". McGraw Hill, (1949)
12. **F. Molland**, "Rudder Design Data for Small Craft". Southampton (1978)

# 19 - APPENDICES

**WEATHER DATA**

	Nautical Miles	Wind Speed	Wind direct.		Nautical Miles	Wind Speed	Wind direct.	
1 Barcelona	733.3	8.0	45.0	5 Rio de Janeiro	502.2	8.0	45.0	
	956.3	8.0	100.0		700.0	8.0	90.0	
	155.6	13.0	40.0		669.6	8.0	160.0	
	356.3	13.0	50.0		1674.1	13.0	110.0	
	233.3	13.0	65.0					
	311.1	13.0	90.0					
Fernando de Noronha	356.3	13.0	140.0	Fernando de Noronha				
				Baltimore /Annapolis	700.0	13.0	0.0	
Cape Town	733.3	8.0	80.0	Inshore	15.0	10.0	0.0	
	1100.0	10.0	100.0		15.0	10.0	45.0	
	1200.0	10.0	170.0		15.0	10.0	180.0	
Inshore	15.0	15.0	0.0	6 Baltimore	100.0	5.0	90.0	
	15.0	15.0	45.0	New York				
	15.0	15.0	180.0					
2 Cape Town	360.0	10.0	160.0	7 New York	538.1	20.0	140.0	
	400.0	20.0	140.0		1614.3	22.0	170.0	
	380.0	20.0	180.0		1076.2	22.0	180.0	
	Kerguelen,	450.0	25.0	150.0	Lizard			
		460.0	27.0	140.0		50.0	15.0	140.0
	Eclipse island	400.0	30.0	150.0	Southampton			
300.0		10.0	160.0	Inshore		15.0	12.0	0.0
860.0		20.0	140.0	15.0		12.0	45.0	
Melbourne	400.0	25.0	110.0	15.0	12.0	180.0		
	890.0	25.0	170.0					
	915.0	30.0	170.0	8 Southampton	154.0	5.0	90.0	
Inshore	15.0	15.0	0.0	100.0	5.0	140.0		
	15.0	15.0	45.0	100.0	10.0	20.0		
	15.0	15.0	180.0	335.0	15.0	90.0		
3 Melbourne	311.0	5.0	0.0	Gothenburg				
	380.0	10.0	170.0		Inshore	15.0	11.0	0.0
	350.0	12.0	90.0		15.0	11.0	45.0	
	320.0	15.0	90.0		15.0	11.0	180.0	
	50.0	20.0	0.0					
4 Wellington	150.0	5.0	40.0	9 Kiel	230.0	5.0	140.0	
	700.0	20.0	90.0					
	435.0	20.0	130.0					
	1565.0	20.0	170.0					
	400.0	25.0	95.0					
	1185.0	25.0	170.0					
Cap horn	700.0	27.0	100.0					
	216.0	5.0	40.0					
	900.0	7.0	170.0					
	500.0	15.0	170.0					
Rio de Janeiro	1064.0	20.0	90.0					
Inshore	15.0	8.0	0.0					
	15.0	8.0	45.0					
	15.0	8.0	180.0					

## Weight and centres estimate

### Weight and centres estimate canting keel 0°

	Weight total	Weight for measurement	X	Y	Z
<b>Structure</b>	2476.73	2476.73	10.68	0.00	0.61
<b>Canting keel mech</b>	369.65	369.65	11.05	0.00	-0.27
<b>Keel</b>	1567.80	1567.80	11.05	0.00	-1.91
<b>Bulb</b>	5820.00	5820.00	11.05	0.00	-4.22
<b>Rudders</b>	54.00	54.00	11.21	0.00	-1.12
<b>Equipment</b>	928.00	928.00	14.67	0.00	0.05
<b>Mast</b>	625.00	625.00	10.74	0.00	13.50
<b>Extra rigging</b>	65.00	65.00	10.85	0.00	4.50
<b>Afloat</b>			12.89	0.00	1.35
<b>Sails</b>	735.51	10.00	-		-
<b>Crew + equipment</b>	950.00	75.00	-		-
<b>Security</b>	200.10	95.23	-		-
<b>Communication</b>	141.30	138.38	-		-
<b>Extra (as specified by rule)</b>	556.70	502.50	-		-
<b>Liquid tanks</b>	571.00	122.50	-		-
<b>Deck equipment</b>	482.90	482.90	14.20	0.00	1.86
	5%	777.18	666.63		
<b>Total</b>	<b>16320.88</b>	<b>13999.33</b>	<b>11.667</b>	<b>0.00</b>	<b>-0.7954</b>

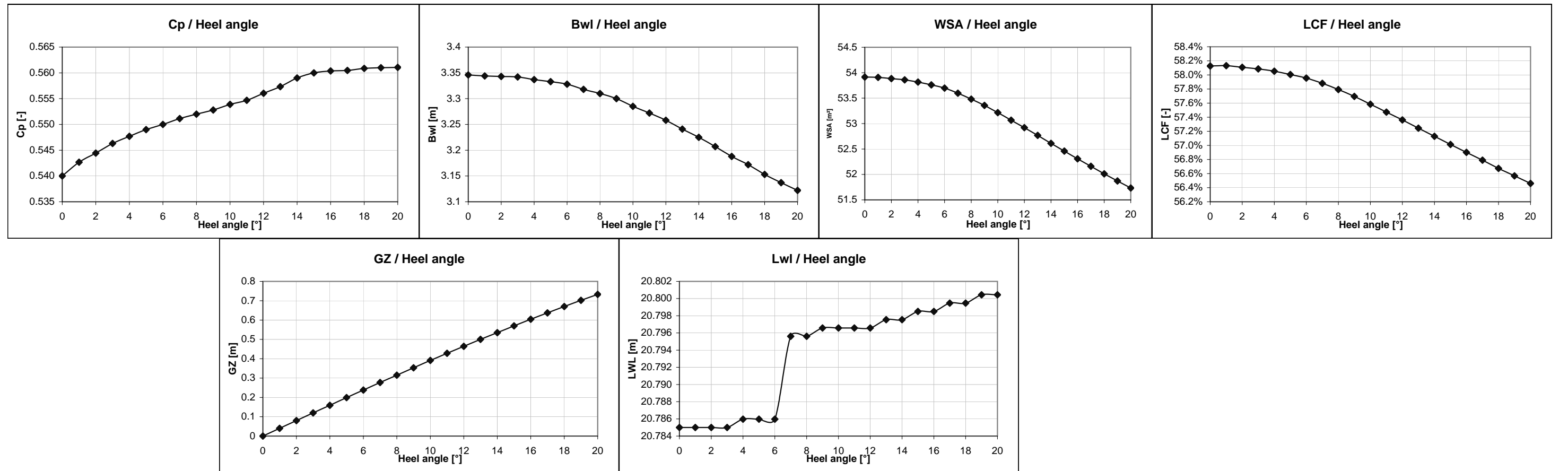
### Weight and centres estimate canting keel 40°

	Weight total	Weight for measurement	X	Y	Z
<b>Structure</b>	2476.73	2476.73	10.68	0.00	0.61
<b>Canting keel mech</b>	369.65	369.65	11.05	0.00	-0.27
<b>Keel</b>	1567.80	1567.80	11.05	0.00	-0.27
<b>Bulb</b>	5820.00	5820.00	11.05	1.17	-1.57
<b>Rudders</b>	54.00	54.00	11.21	2.47	-3.40
<b>Equipment</b>	928.00	928.00	14.67	0.00	0.05
<b>Mast</b>	625.00	625.00	10.74	0.00	13.50
<b>Extra rigging</b>	65.00	65.00	10.85	0.00	4.50
<b>Afloat</b>			12.89	0.00	1.35
<b>Sails</b>	735.51	10.00	-		-
<b>Crew + equipment</b>	950.00	75.00	-		-
<b>Security</b>	200.10	95.23	-		-
<b>Communication</b>	141.30	138.38	-		-
<b>Extra (as specified by rule)</b>	556.70	502.50	-		-
<b>Liquid tanks</b>	571.00	122.50	-		-
<b>Deck equipment</b>	482.90	482.90	14.20	0.00	1.86
	5%	777.18	666.63		
<b>Total</b>	<b>16320.88</b>	<b>13999.33</b>	<b>11.667</b>	<b>0.97</b>	<b>-0.465</b>

HULL HYDROSTATIC DATA RACING DISPLACEMENT 16320 kg

Racing displacement 16.32t

Heel angle	0	1	2	3	4	5	6	7	8	9	10	11	12	13	14	15	16	17	18	19	20
Draft at FP m	2.519	2.518	2.519	2.52	2.52	2.521	2.522	2.524	2.525	2.527	2.528	2.53	2.532	2.535	2.537	2.539	2.541	2.544	2.546	2.549	2.551
Draft at AP m	2.509	2.509	2.507	2.504	2.5	2.496	2.49	2.483	2.475	2.467	2.457	2.446	2.434	2.421	2.407	2.392	2.376	2.36	2.342	2.323	2.303
WL Length m	20.785	20.785	20.785	20.785	20.786	20.786	20.786	20.796	20.796	20.797	20.797	20.797	20.797	20.798	20.798	20.799	20.799	20.799	20.799	20.800	20.800
Immersed Depth m	0.598	0.598	0.599	0.6	0.602	0.604	0.607	0.609	0.612	0.615	0.618	0.621	0.625	0.628	0.632	0.635	0.639	0.642	0.645	0.649	0.652
WL Beam m	3.346	3.344	3.343	3.342	3.337	3.333	3.328	3.318	3.31	3.3	3.285	3.272	3.258	3.241	3.225	3.207	3.188	3.172	3.153	3.137	3.122
Wetted Area m^2	53.914	53.907	53.884	53.86	53.816	53.761	53.697	53.598	53.48	53.357	53.215	53.067	52.92	52.768	52.611	52.459	52.308	52.16	52.012	51.872	51.733
Waterpl. Area m^2	48.571	48.564	48.536	48.509	48.456	48.392	48.318	48.201	48.065	47.924	47.76	47.581	47.403	47.217	47.027	46.84	46.654	46.47	46.288	46.116	45.945
Cp	0.540	0.543	0.544	0.546	0.548	0.549	0.550	0.551	0.552	0.553	0.554	0.555	0.556	0.557	0.559	0.560	0.560	0.560	0.561	0.561	0.561
VCB from DWL m	0.209	0.209	0.209	0.209	0.209	0.21	0.21	0.21	0.211	0.211	0.212	0.213	0.213	0.214	0.215	0.216	0.217	0.218	0.218	0.219	0.22
GZ m	0	0.04	0.08	0.12	0.159	0.199	0.238	0.277	0.315	0.353	0.391	0.428	0.464	0.5	0.535	0.57	0.604	0.637	0.67	0.702	0.733
LCF to Amidsh. m	58.13%	58.13%	58.11%	58.09%	58.05%	58.01%	57.96%	57.88%	57.79%	57.70%	57.58%	57.47%	57.36%	57.24%	57.13%	57.01%	56.90%	56.79%	56.67%	56.57%	56.46%
TCF to zero pt. m	0	-0.03	-0.059	-0.089	-0.119	-0.148	-0.178	-0.207	-0.235	-0.263	-0.29	-0.317	-0.344	-0.369	-0.395	-0.42	-0.444	-0.468	-0.491	-0.514	-0.537





```

plot(cos(angel.*pi/180).*b,chord,'--
rs','LineWidth',2,...
    'MarkerEdgeColor','k',...
    'MarkerFaceColor','g',...
    'MarkerSize',5)
title('chord dist')
axis([0 b 0 cr*1.1])

% downwash distribution
% page 278

% with uinf=1
dwash=uinf*(A1 + 3*A3.*sani3./sani+
5*A5.*sani5./sani+ 7*A7.*sani7./sani+
9*A9.*sani9./sani+ 11*A11.*sani11./sani+
13*A13.*sani13./sani+ 15*A15.*sani15./sani...
+
17*A17.*sani17./sani);
dw=[cos(angel.*pi/180)',dwasht'];
figure(3)
plot(dw(:,1),dw(:,2),'--rs','LineWidth',2,...

```

```

    'MarkerEdgeColor','k',...
    'MarkerFaceColor','g',...
    'MarkerSize',5)
title('dw dist')
xlabel('-y/s')
ylabel('dw')

%local cl plot
cla=2.*circ./chord;
cld=[cos(angel.*pi/180)',cla'];

figure(4)
plot(cld(:,1),cld(:,2)./CL,'--
rs','LineWidth',2,...
    'MarkerEdgeColor','k',...
    'MarkerFaceColor','g',...
    'MarkerSize',5)
title('cl dist')
xlabel('-y/s')
ylabel('cl/CL')

```

## ABS RUDDER STOCKS CALCULATION page 1

Project Name **VOLVO 070**

Rudders characteristics	
Clr	1.2 =1.5 for rudders having h/c <6 and t/c>0.06
Lwl	21.5
Arudder	1.2
Chord	0.4 m
Lc	0.05 m

Bearing distance	
Distance 1st 2nd bearing	1 m
Distance 2nd bearing tip	3 m
Lever	1.272 m

Stock materials	
T 800	
ta fibre ud	130 1275 Mpa
ta bx	25 245.3 Mpa
coeff	1.3
ta pratique	79.81 782.9 Mpa
Shear	38.46 Mpa

Disp kg	15000		
coeff	1509.301068		
N	2.014011539	speed assumed	18.07701 knots
Nused	2.717985968	speed used	21 knots
		Fn	0.744396
<b>1. Rudder side force</b>		<b>82802.4641 N</b>	
<b>2. Rudder torsionnal moment</b>		<b>4140.1232 N.m</b>	
<b>3. Rudder bending moment</b>		<b>105324.734 N.m</b>	at 2nd bearing

Force in 1st bearing	126428 N
Force in 2nd bearing	228131 N

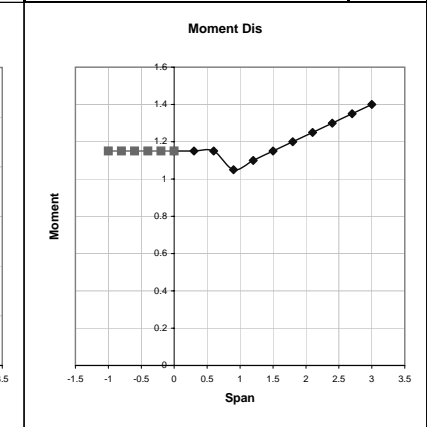
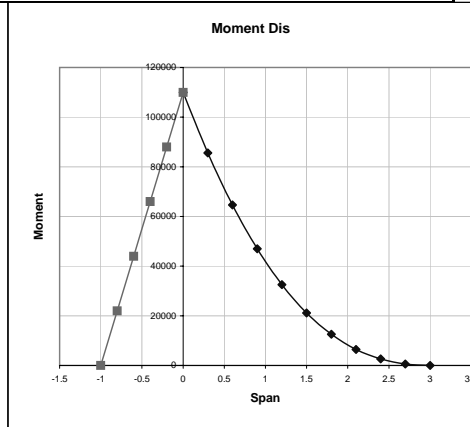
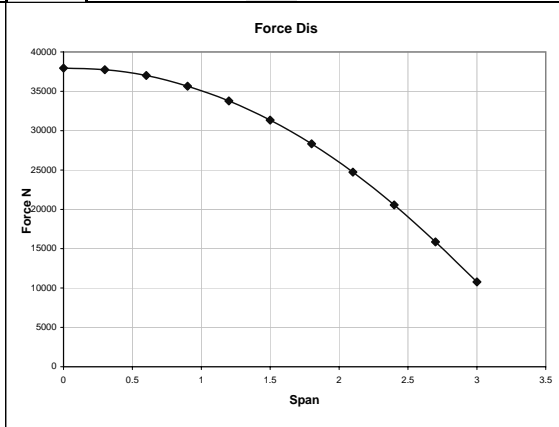
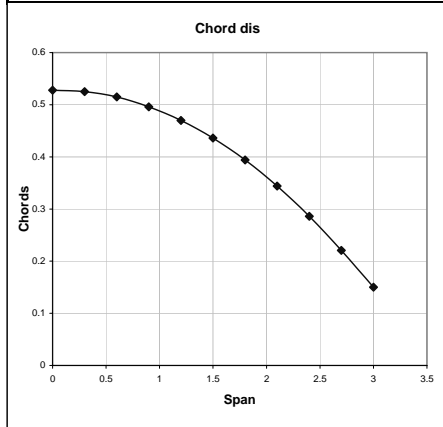
Stock in boat		
0	-1	0
0.2	-0.8	21987.5
0.4	-0.6	43975.1
0.6	-0.4	65962.6
0.8	-0.2	87950.2
1	0	109938

SP system coeff for rudder stock breakage		
Span	Coeff	Moment
-1	1.15	0
-0.8	1.15	25285.68
-0.6	1.15	50571.36
-0.4	1.15	75857.04
-0.2	1.15	101142.7
0	1.15	126428.4
0.3	1.15	98437.72
0.6	1.15	74339.65
0.9	1.05	49355.54
1.2	1.1	35821.12
1.5	1.15	24324.23
1.8	1.2	15055.04
2.1	1.25	8095.073
2.4	1.3	3404.216
2.7	1.35	809.5558
3	1.4	0

All that part will be over build anyway

Rudder chord distribution			
Span	Chord	Area	
0	0	0.528	0.15795
0.1	0.3	0.525	0.156
0.2	0.6	0.515	0.15165
0.3	0.9	0.496	0.1449
0.4	1.2	0.47	0.1359
0.5	1.5	0.436	0.1245
0.6	1.8	0.394	0.1107
0.7	2.1	0.344	0.0945
0.8	2.4	0.286	0.07602
0.9	2.7	0.2208	0.05562
1	3	0.15	1.20774

Elliptical pressure CL= 1.2											
Force N/m	Moment										
37951.13	11394	13933	15283	15516	14765	13187	10936	8175	5046	1703	<b>109938</b>
37735.5	10194	12294	13245	13129	12081	10257	7811	4905	1682		<b>85598</b>
37016.73	8995	10655	11207	10742	9396	7326	4687	1635			<b>64643</b>
35651.06	7796	9016	9170	8355	6712	4396	1562				<b>47005</b>
33782.26	6596	7377	7132	5968	4027	1465					<b>32565</b>
31338.43	5397	5737	5094	3581	1342						<b>21152</b>
28319.59	4198	4098	3057	1194							<b>12546</b>
24725.74	2998	2459	1019								<b>6476</b>
20556.86	1799	820									<b>2619</b>
15870.47	600										<b>600</b>
10781.57											<b>0</b>



span	Force per m	Action	Force
0	43643.8	0.15	13055.9432
0.3	43395.8	0.45	12894.7587
0.6	42569.2	0.75	12000.4274
0.9	37433.6	1.05	11189.1142
1.2	37160.5	1.35	10979.9517
1.5	36039.2	1.65	10503.4063
1.8	33983.5	1.95	9733.60215
2.1	30907.2	2.25	8644.6635
2.4	26723.9	2.55	7222.35867
2.7	21425.1	2.85	5477.90051
3	15094.2		

101702.126

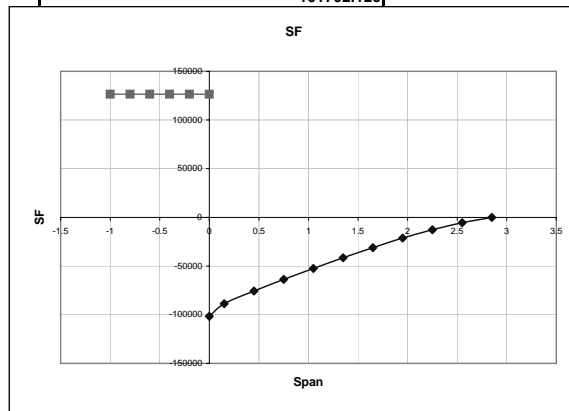
SF	
-1	126428.4
-0.8	126428.4
-0.6	126428.4
-0.4	126428.4
-0.2	126428.4
0	126428.4
0	-101702
0.15	-88646
0.45	-75751
0.75	-63751
1.05	-52562
1.35	-41582
1.65	-31079
1.95	-21345
2.25	-12700
2.55	-5478
2.85	0

Span	Moment [N.m]	Zmin [cm3]	Chord	y [cm]	I [cm4]	Area SF [mm²]
-1	0.00	0.00		3.168	0	3287
-0.8	25285.68	32.30		3.168	102.3166	3287
-0.6	50571.36	64.59		3.168	204.6332	3287
-0.4	75857.04	96.89		3.168	306.9498	3287
-0.2	101142.72	129.19		3.168	409.2663	3287
0	126428.40	161.48	0.528	3.168	511.5829	3287
0.3	98437.72	125.73	0.525	3.15	396.0576	2644
0.6	74339.65	94.95	0.515	3.09	293.4035	2305
0.9	49355.54	63.04	0.496	2.976	187.6096	1970
1.2	35821.12	45.75	0.47	2.82	129.0252	1658
1.5	24324.23	31.07	0.436	2.616	81.27613	1367
1.8	15055.04	19.23	0.394	2.364	45.45856	1081
2.1	8095.07	10.34	0.344	2.064	21.34109	808
2.4	3404.22	4.35	0.286	1.716	7.461406	555
2.7	809.56	1.03	0.2208	1.3248	1.369883	330
3	0.00	0.00	0.15	0.9	0	142

I [cm4]	y [cm]	Zmin [cm3]	Area [mm²]
249.00	3.57	69.75	4915
310.00	3.67	84.47	5217
381.00	3.78	100.79	6766
475.00	3.87	122.74	8851
565.00	4.02	140.55	9215
721.00	4.225	170.65	9826
525.42	3.93	133.66	-
381.43	3.78	100.82	-
248.59	3.61	68.93	-
187.93	3.50	53.69	-
101.13	3.21	31.50	-
36.99	2.82	35.93	-
6.91	2.20	14.55	-
		11.41	-
		22.81	-
		5.11	-

Blade support

True FOS
-
301%
179%
146%
125%
122%
122%
115%
129%
117%
224%
176%
341%
2978%
-



Blade carbon

	I [cm4]	y [cm]	Zmin [cm3]
T blade plate 2.3mm = 1500gcarbon			
Blade t 60cm	224.541	4.225	53.1457988
Blade t 40cm	64.2146	2.815	22.8115808
Blade t 20cm	7.2119	1.41	5.1148227

**KEEL CALCS**

INPUT DATA	
Bulb Weight	5820 kg
Bulb lever	3674 mm
Bulb lever at end	274 mm
Keel weight	1567.8 kg
Keel lever	1800 mm
Yield strength	390 MPa
FOS	3 MPa
Allowed strength	130 MPa

**SECTION CALCS**

Coordinate	BM [kN.m]	Zmin[cm <sup>4</sup> ]	Iachieved	Yachieved	Zachieved	Zachieved /Zmin	t	c	t/c
0	261.8	2013.71	17873.64	8.99	2127.34	106%	17.92	81.5	0.22
500	222.1	1708.49	13842.07	8.65	1712.26	100%	17.4	79.1	0.22
1000	183.7	1413.46	11081.87	8.18	1449.58	103%	16.56	75.3	0.22
1500	146.7	1128.13	8249.50	7.56	1167.59	103%	15.52	70.5	0.22
2000	110.7	851.89	5611.55	6.78	885.60	104%	14.14	64.6	0.22
2500	75.9	583.97	3387.43	5.86	618.52	106%	12.48	57.7	0.22
3000	42.1	323.49	1721.22	4.79	384.49	119%	10.54	50.2	0.21
3400	15.6	120.34	825.29	3.82	231.17	192%	8.76	43.7	0.20

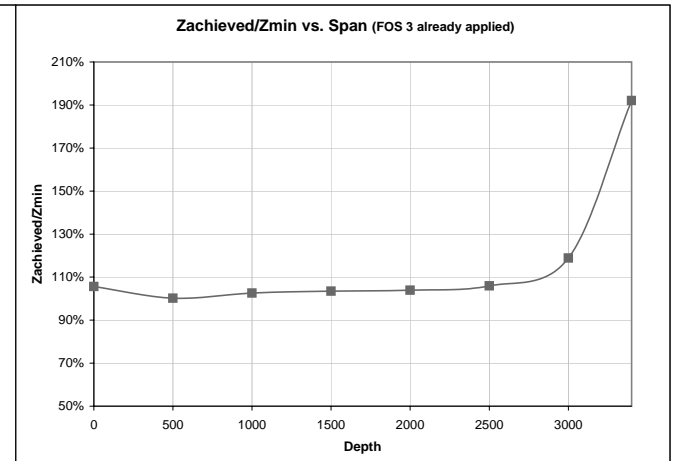
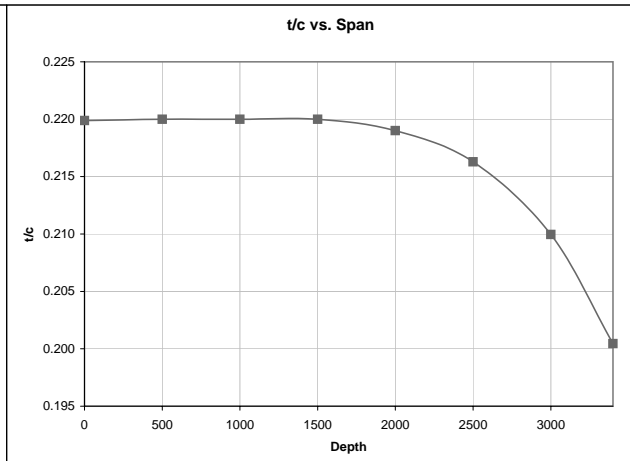
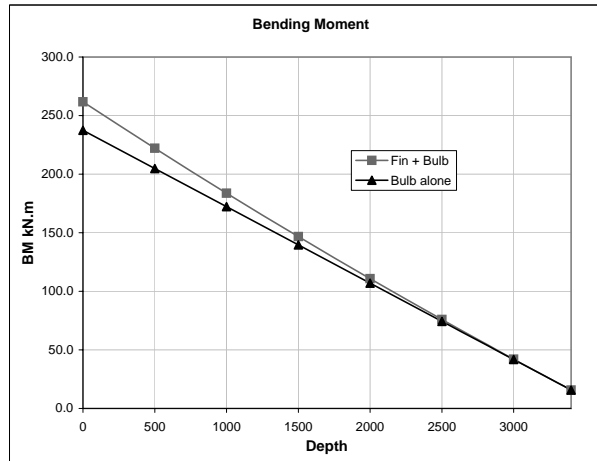
Total volume	0.201
after 3d modelling	7800
Weight	1567.8 kg

**BM CALCS**

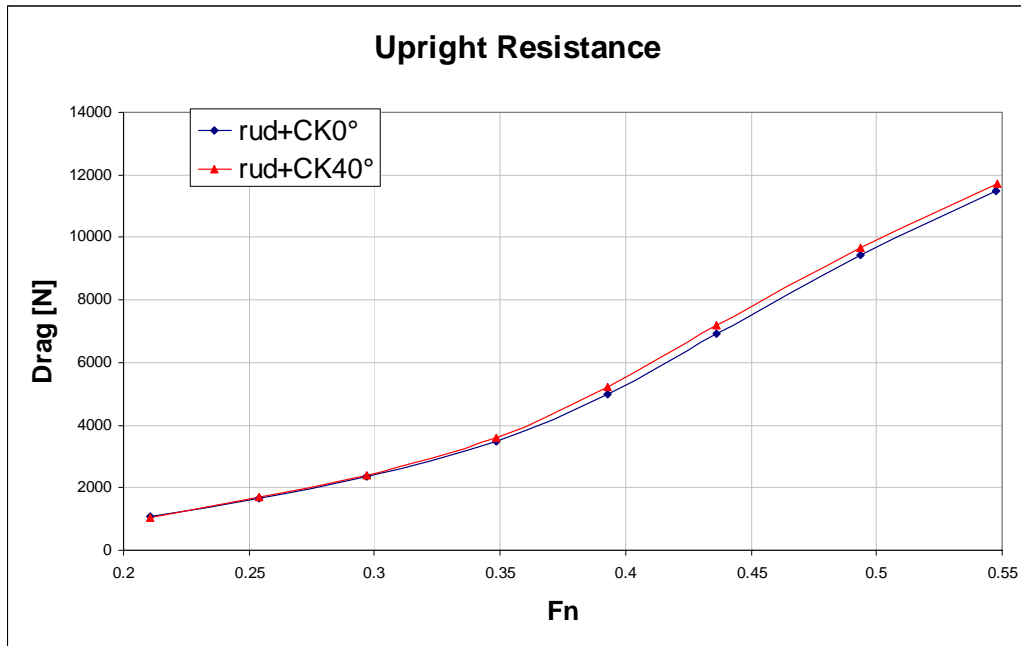
Max BM	237.4 kN.m	@	0
BM at end	15.6 kN.m	@	3400

Average chord	Mass [N]	Lever	BM due to fin	BM due to bulb	BM total
80.295455	2700.808	250	24.33	237.45	261.78
77.181818	2596.078	750	17.27	204.83	222.10
72.909091	2452.361	1250	11.54	172.21	183.75
67.555832	2272.3	1750	7.06	139.59	146.66
61.133105	2056.266	2250	3.77	106.98	110.75
53.95	1814.655	2750	1.56	74.36	75.92
46.95	1579.204	3200	0.32	41.74	42.05
			0.00	15.64	15.64

Chord average	65.322
Weight/part	223.971 1577
Weight/part/chord av	3.429

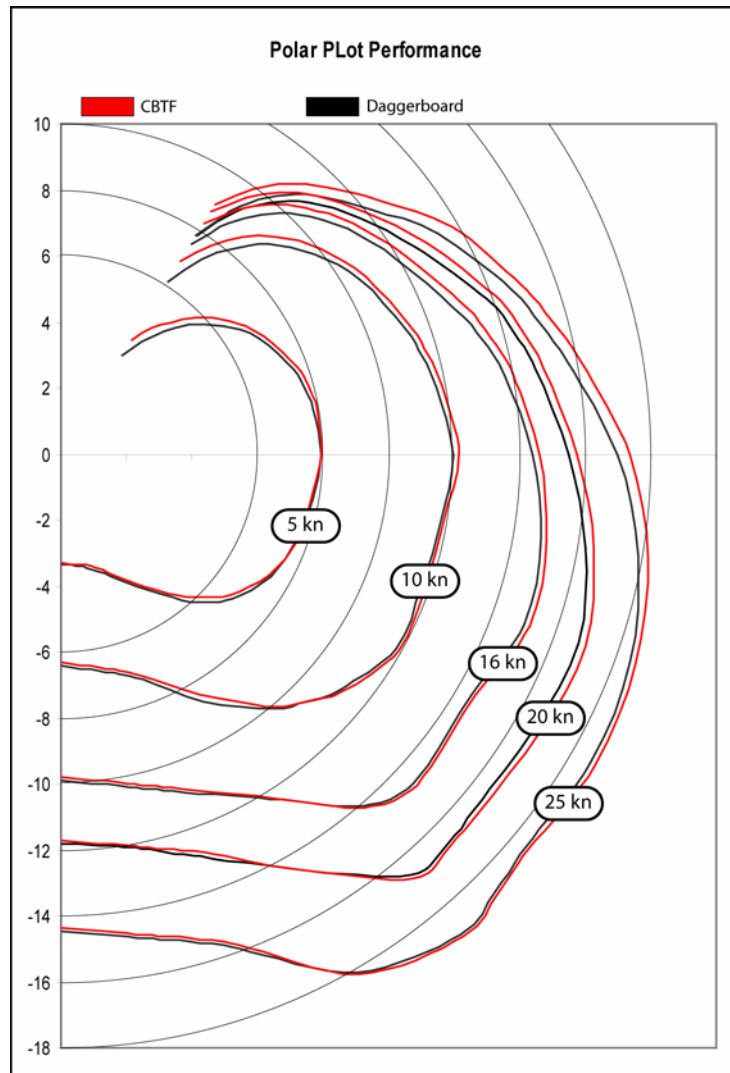


Towing tank



Graph 19.a

VPP comparison



Rig Design

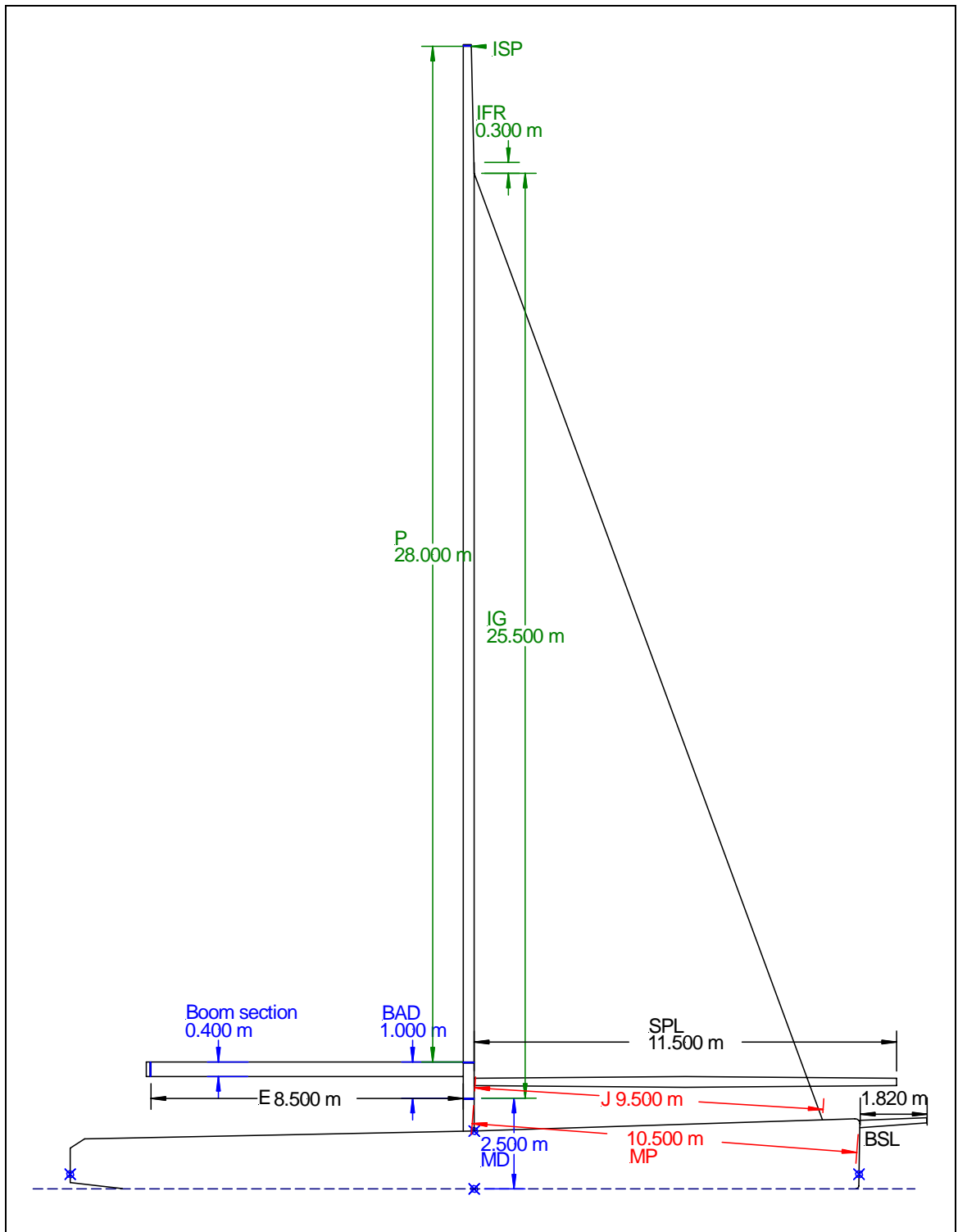


Figure 19.a – Rig measurement

## Sail design

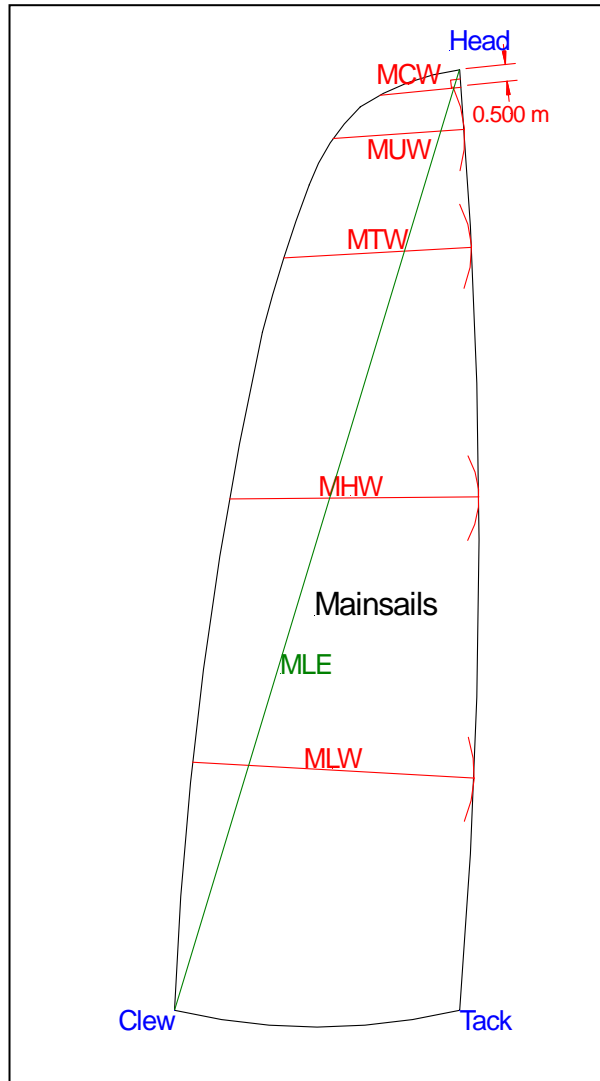


Figure 19.b - Sail measurement

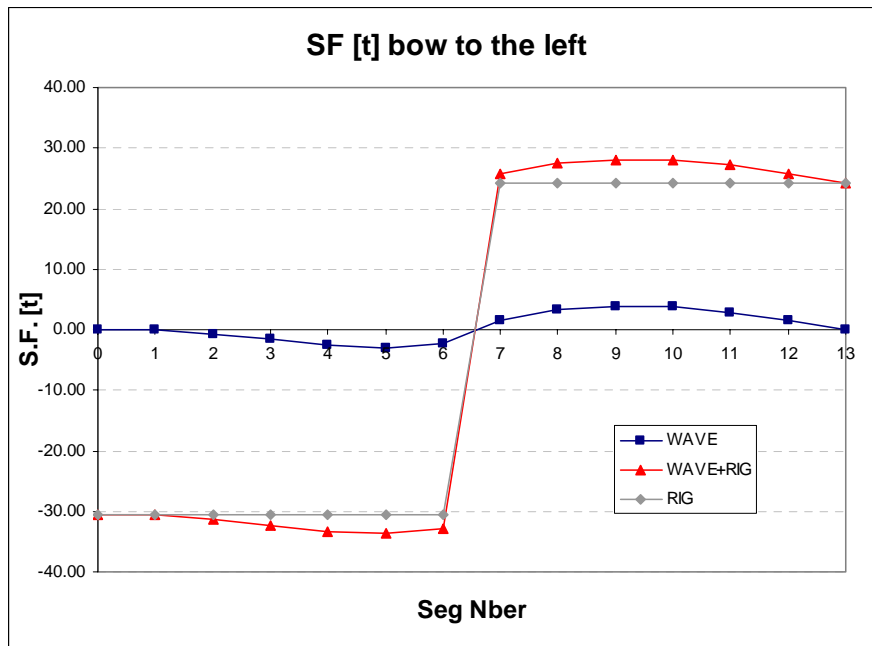
### ABS Internals Sample Calcs

SM base											
Item	Type	C	I	Cf	F	Multiplier	h	s	oa	SM	Smachieved
			[m]			h	[m]	[m]	/mm'	[cm^3]	[cm^3]
#L1 Longi	Longi	817	3.824	2.0868	0.250	1.08	1.457	1.3	163	138.79	180.12
#L1 Longi	Longi	817	1.86	0.9388	0.267	1.08	1.554	1.4	163	37.727	180.12
#L1 Longi	Longi	817	3.833	2.0921	0.250	1.08	1.457	1.6	163	171.63	180.12
#L1 Longi	Longi	817	0.97	0.4185	0.558	1.08	3.250	1.229	163	18.84	180.12
#L1 Longi	Longi	817	3.636	1.9769	0.250	1.0215	1.378	1.229	163	112.2	180.12
#L1 Longi	Longi	817	1.839	0.9265	0.270	0.9405	1.370	1.229	163	28.541	180.12
#L1 Longi	Longi	817	4.386	2.4153	0.250	0.864	1.165	1.229	163	138.09	180.12
#L2 Longi	Longi	817	2.063	1.0574	0.250	1.2	1.739	0.9	163	33.377	72.7
#L2 Longi	Longi	817	0.63	0.2198	0.747	1.2	5.193	1.3	163	13.43	115.2
#L2 Longi	Longi	817	3.8	2.0728	0.250	1.2	1.739	1.7	163	213.91	220.2
#L2 Longi	Longi	817	2.919	1.5578	0.250	1.2	1.739	1.7	163	126.22	140.63
#LD1 longi	Longi	817	6.35	3.563349	0.25	1	0.67	0.7	163	94.788	100.98
#LD1 longi	Longi	817	3.8	2.072775	0.25	1	0.67	1.7	163	82.438	100.98
#LD1 longi	Longi	817	0.9	0.377612	0.593397	1	1.5903	1.7	163	10.976	100.98
#LD1 longi	Longi	817	1.8	0.903697	0.276583	1	0.74124	1.7	163	20.464	100.98
#A1 Trans	Longi	817	1.594	0.783282	0.321502	1.2	2.08141	1.4	163	37.11	38.54
#A1 Trans	Longi	817	0.897	0.375859	0.594959	1.2	4.13734	1.4	163	23.36	38.54
#A1 Trans	Longi	817	0.897	0.375859	0.594959	1.2	4.13734	1.4	163	23.36	38.54
#A1 Trans	Longi	817	1.594	0.783282	0.321502	1.2	2.08141	1.4	163	37.11	38.54
Deck Trans	Longi	817	0.856		0.7596		2.47566	1.4	163	12.729	38.54
Deck Trans	Longi	817	0.856		0.7596		2.47566	1.4	163	12.729	38.54
#A2 Trans	Longi	817	1.504	0.730674	0.346411	1.2	2.24267	1.4	163	35.598	38.54
#A2 Trans	Longi	817	0	-0.14847	1	1.2	6.954	1.4	163	0	38.54
#A2 Trans	Longi	817	0	-0.14847	1	1.2	6.954	1.4	163	0	38.54
#A2 Trans	Longi	817	1.504	0.730674	0.346411	1.2	2.24267	1.4	163	35.598	38.54
Deck Trans	Longi	817	1.146		0.6436		2.37706	1.4	163	21.906	38.54
Deck Trans	Longi	817	1.146		0.6436		2.37706	1.4	163	21.906	38.54
#A3 Trans	Longi	817	1.626	0.801987	0.313414	1.2	2.02904	1.4	163	37.644	38.54
#A3 Trans	Longi	817	1.411	0.676312	0.375468	1.2	2.611	1.4	163	36.477	38.54
#A3 Trans	Longi	817	1.411	0.676312	0.375468	1.2	2.611	1.4	163	36.477	38.54
#A3 Trans	Longi	817	1.626	0.801987	0.313414	1.2	2.02904	1.4	163	37.644	38.54
Deck Trans	Longi	817	1.802		0.3812		2.15402	1.4	163	49.082	50.12
Deck Trans	Longi	817	1.802		0.3812		2.15402	1.4	163	49.082	50.12
#A4 Trans	Longi	817	1.262	0.589215	0.428943	1.2	2.77698	1.917	163	42.496	52.12
#A4 Trans	Longi	817	1.192	0.548298	0.456967	1.2	3.17775	1.917	163	43.384	52.12
#A4 Trans	Longi	817	1.796	0.901359	0.277293	1.2	1.92829	1.917	163	59.764	62.47
#A4 Trans	Longi	817	1.192	0.548298	0.456967	1.2	3.17775	1.917	163	43.384	52.12
#A4 Trans	Longi	817	1.262	0.589215	0.428943	1.2	2.77698	1.917	163	42.496	52.12
Deck Trans	Longi	817	1.336		0.5676		2.31246	1.917	163	39.659	52.12
Deck Trans	Longi	817	0.941		0.7256		2.44676	1.917	163	20.817	52.12
Deck Trans	Longi	817	1.336		0.5676		2.31246	1.917	163	39.659	52.12
Deck Trans	Longi	817	0.941		0.7256		2.44676	1.917	163	20.817	52.12
#A5 Trans	Longi	817	0.73	0.278241	0.686967	1.2	4.44743	1.917	163	22.773	52.12
#A5 Trans	Longi	817	0.6	0.20225	0.765341	1.2	5.32218	1.917	163	18.41	52.12
#A5 Trans	Longi	817	1.752	0.875639	0.285529	1.2	1.98557	1.917	163	58.561	67.85
#A5 Trans	Longi	817	0.6	0.20225	0.765341	1.2	5.32218	1.917	163	18.41	52.12
#A5 Trans	Longi	817	0.73	0.278241	0.686967	1.2	4.44743	1.917	163	22.773	52.12
Deck Trans	Longi	817	0.795		0.784		2.4964	1.917	163	15.16	52.12
Deck Trans	Longi	817	0.727		0.8112		2.51952	1.917	163	12.795	52.12
Deck Trans	Longi	817	0.55		0.882		2.5797	1.917	163	7.4981	52.12
Deck Trans	Longi	817	1.796		0.3836		2.15606	1.917	163	66.824	67.85
Deck Trans	Longi	817	0.795		0.784		2.4964	1.917	163	15.16	52.12
Deck Trans	Longi	817	0.727		0.8112		2.51952	1.917	163	12.795	52.12
Deck Trans	Longi	817	0.55		0.882		2.5797	1.917	163	7.4981	52.12

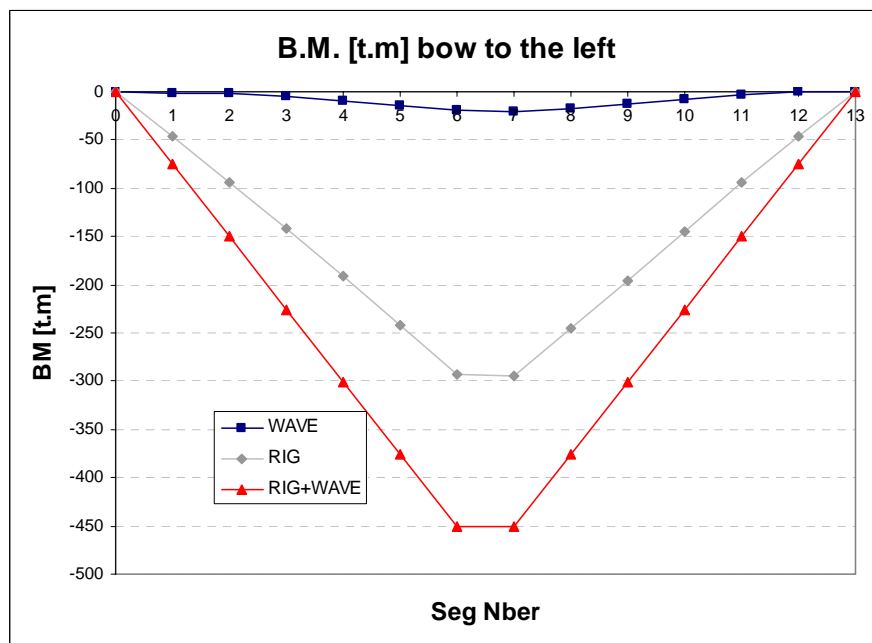
#A6 Trans	Longi	817	0.835	0.339617	0.627966	1.2	4.06545	1.917	163	27.236	52.12
#A6 Trans	Longi	817	0.651	0.232062	0.733899	1.2	5.10353	1.917	163	20.782	52.12
#A6 Trans	Longi	817	1.758	0.879147	0.28436	1.2	1.97744	1.917	163	58.721	67.85
#A6 Trans	Longi	817	0.651	0.232062	0.733899	1.2	5.10353	1.917	163	20.782	52.12
#A6 Trans	Longi	817	0.835	0.339617	0.627966	1.2	4.06545	1.917	163	27.236	52.12
Deck Trans	Longi	817	0.795		0.784		2.4964	1.917	163	15.16	52.12
Deck Trans	Longi	817	0.727		0.8112		2.51952	1.917	163	12.795	52.12
Deck Trans	Longi	817	0.55		0.882		2.5797	1.917	163	7.4981	52.12
Deck Trans	Longi	817	1.796		0.3836		2.15606	1.917	163	66.824	67.85
Deck Trans	Longi	817	0.795		0.784		2.4964	1.917	163	15.16	52.12
Deck Trans	Longi	817	0.727		0.8112		2.51952	1.917	163	12.795	52.12
Deck Trans	Longi	817	0.55		0.882		2.5797	1.917	163	7.4981	52.12

#B1 Trans	Longi	817	2.365	1.233962	0.25	1.2	1.7385	2.3	163	112.1	128.6
#B1 Trans	Longi	817	1.795	0.900775	0.277471	1.2	1.92953	2.3	163	71.671	89
#B1 Trans	Longi	817	2.365	1.233962	0.25	1.2	1.7385	2.3	163	112.1	128
Deck Trans	Longi	817	1.078		0.6708		2.40018	2.3	163	32.155	70
Deck Trans	Longi	817	2.132		0.33		2.1105	2.3	163	110.59	128
Deck Trans	Longi	817	1.078		0.6708		2.40018	2.3	163	32.155	70

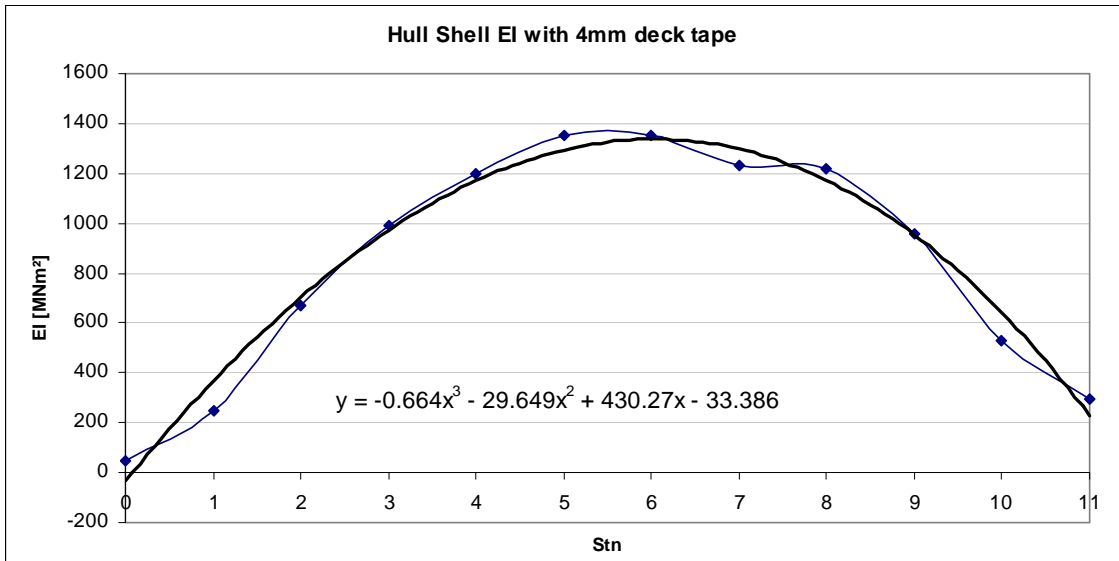
## Hull Structural design



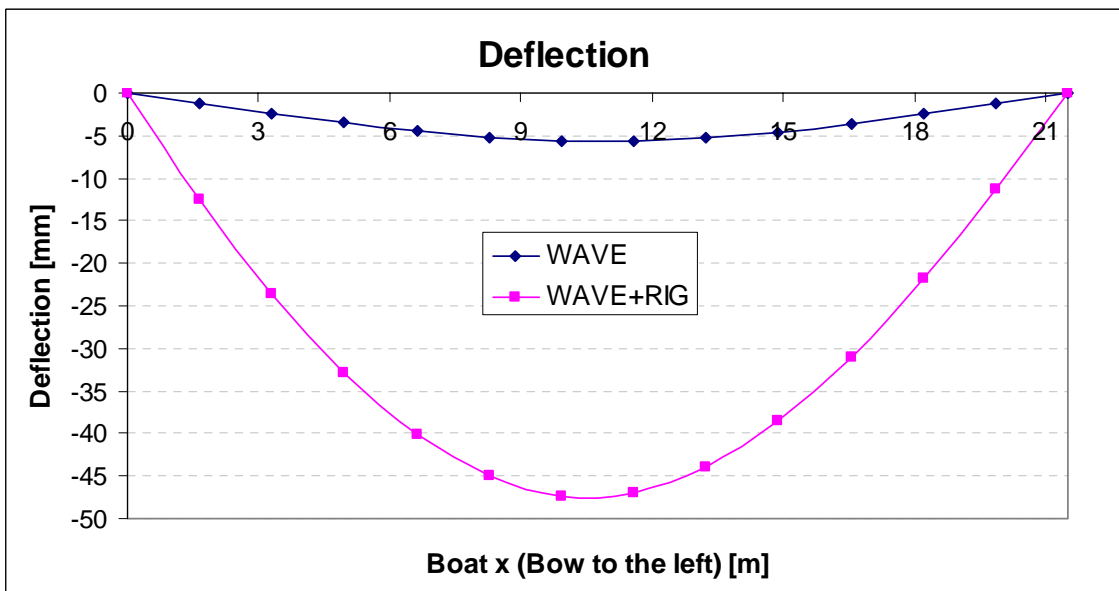
Graph 19.b Shear Force due to global loads



Graph 19.c Bending moment due to global loads



Graph 19.d Hull shell EI with 4mm UD tape on deck



Graph 19.e Hull deflections under global loads